Journal of Hydrology 621 (2023) 129585

Contents lists available at ScienceDirect

Journal of Hydrology

journal homepage: www.elsevier.com/locate/jhydrol

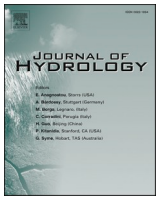

Research papers

Modeling wildfire effects on streamflow in the Cascade Mountains, Oregon, USA

K.A. Wampler [a,*], K.D. Bladon [a], M. Faramarzi [b]

[a] Department of Forest Engineering, Resources, and Management, Oregon State University, Corvallis, OR 97331, USA
[b] Watershed Science and Modelling Laboratory, Department of Earth and Atmospheric Sciences, University of Alberta, Edmonton, AB T6G 2E3, Canada

ARTICLE INFO

Keywords:
Wildfire
Oregon
Source water
Hydrologic model
Streamflow

ABSTRACT

Increasing occurrence of large and severe wildfires represents a growing threat to forested watersheds and the many ecosystem services they provide. Past research has shown that wildfires can cause substantial increases in peak flows and annual water yields, leading to potential water quality concerns and land and water management challenges. However, responses have been variable, and there have been few studies at large basin scales, leading to uncertainties about post-fire hydrologic responses. To address these uncertainties, we projected the effect of three large wildfires (>70,000 ha) on streamflow in two important forested watersheds in the Cascade Range of Oregon, US. We modeled the streamflow response using the Soil and Water Assessment Tool (SWAT) model, calibrated on data from prior to the wildfires. We modified model parameters to represent the impacts of the wildfires based on burn severity maps. Burned and unburned scenarios were compared using random forest models to identify drivers of increased annual water yields and peak flows. Post-fire annual water yield changes were controlled by burn severity, annual precipitation, area burned, aridity, and vegetation type, while post-fire peak flow changes were controlled by burn severity, area burned, aridity, soil type, and geologic province. We also found that post-fire increases in annual water yields, peak flows, and low flows were greatest at the headwater scale but were more muted at the downstream basin scale. Our work provides valuable insights into the range of potential post-fire streamflow changes at the headwater and larger basin scale, which is becoming increasingly critical for effective forest and water management decisions.

1. Introduction

Forested basins are critical sources of drinking water, providing water supplies to almost one-third of the world's largest cities and two-thirds of cities in the United States (US) (Committee on Hydrologic Impacts of Forest Management, 2008; Dudley and Stolton, 2003). Healthy forests are naturally effective at filtering and storing water, which are services that save an estimated $25.9-billion dollars worldwide every year (Costanza et al., 1997). However, healthy source water supplies are increasingly at risk due to growing pressures from urbanization (Paul and Meyer, 2001; Walsh et al., 2005), deforestation (Warziniack et al., 2017), climate change (Delpla et al., 2009; Murdoch et al., 2000), extreme weather events (Khan et al., 2015), forest pathogens (Bladon et al., 2019), pest outbreaks (Kurz et al., 2008; Mikkelson et al., 2013), and wildfire (Bladon et al., 2014; Hohner et al., 2019). As a result, water crises, or significant issues with streamflow and water quantity, have been identified as representing one of the greatest global risks that could negatively impact society (Martin, 2016; World Economic Forum, 2015). Therefore, it is critical to improve our understanding of the variability and drivers of source water changes from these growing pressures.

In particular, there is increasing concern about the effects of wildfire on surface source water supplies (Bladon, 2018; Hallema et al., 2018; Martin, 2016; Robinne et al., 2021) due to recent and dramatic increases in the timing, extent, and severity of wildfire activity in many regions of the world (Flannigan et al., 2009; Moritz et al., 2012; Reilly et al., 2017). Historical evidence and modeling efforts suggest that we will continue to observe years with elevated fire danger, contributing to longer fire seasons and increased burned area (Abatzoglou et al., 2021; Flannigan et al., 2013; Murphy et al., 2018). In part, the increase in area burned is attributable to warmer temperatures, earlier spring snowmelts, increased fuel aridity, and greater fuel accumulation (Abatzoglou et al., 2018; Marlon et al., 2012; Westerling, 2016). Indeed, in recent years, many areas around the globe have experienced some of their most

* Corresponding author at: 216 Peavy Forest Science Center, Department of Forest Engineering, Resources, and Management, Corvallis, OR 97331, USA.
E-mail address: katie.wampler@oregonstate.edu (K.A. Wampler).

https://doi.org/10.1016/j.jhydrol.2023.129585
Received 23 March 2022; Received in revised form 20 April 2023; Accepted 23 April 2023
Available online 27 April 2023

destructive wildfire seasons in recorded history. For example, in 2020, 2.9-million ha burned in California, Washington, and Oregon alone—29 % of the total area burned in the US that year. Across the entire US, the area burned in 2020 was 2.1-times greater than the long-term average (Congressional Research Service, 2021; Geographic Area Coordination Center, 2020; National Interagency Fire Center, n.d.). Similarly, the 2019–2020 wildfire season in Australia burned almost 19-million ha, consuming ~21 % of the temperate forest biome in that region, primarily in New South Wales and Victoria (Boer et al., 2020; Filkov et al., 2020). In 2017 and 2018, wildfires in British Columbia, Canada burned 3.3- to 3.7-times more area than the 10-year average (2009–2019) (BC Wildfire Service, n.d.). In Europe, many countries, including Spain, Italy, Portugal, Sweden, and the UK have all experienced notable wildfire seasons in recent years (Henley and Jones, 2019; San-Miguel-Ayanz et al., 2020).

Recent empirical studies have illustrated that wildfires can cause large and long-lasting effects on a wide range of hydrological processes (Niemeyer et al., 2020; Poon and Kinoshita, 2018; Rhoades et al., 2019). For example, wildfires can impact soil hydraulic properties, reducing infiltration rates and changing water partitioning between surface and subsurface flow (Ebel and Moody, 2017; Moody et al., 2016; Moody and Ebel, 2014). Additionally, the presence of ash, water repellent layers in the soil, surface sealing, and reduced ground cover can contribute to increased occurrence of surface runoff (Balfour et al., 2014; Bodí et al., 2012; Certini, 2005; Larsen et al., 2009; Lavee et al., 1995). Combined with reduced interception losses and higher net precipitation (Kusaka et al., 1983; Ma et al., 2020; Stoof et al., 2012; Williams et al., 2019), these effects often lead to increased annual water yields and peak flows, and changes to the timing of water availability, with effects potentially lasting for multiple decades (Coombs and Melack, 2013; Hallema et al., 2017a; Niemeyer et al., 2020; Wagenbrenner et al., 2021).

Post-fire changes to annual water yields across a number of regions and basin sizes have been observed to range from no change up to a 450 % increase (Bart, 2016; Bart and Hope, 2010; Campbell et al., 1977, 1977; Hallema et al., 2017b; Helvey, 1980; Loáiciga et al., 2001; Mahat et al., 2016; Niemeyer et al., 2020; Owens et al., 2013; Scott, 1997; Wine and Cadol, 2016). Wildfire can also affect both peak flows and low flows. Peak and storm flows have been found to increase between 20 % and 290 % in Alberta, CAN, Washington, US, and South Africa (Mahat et al., 2016; Niemeyer et al., 2020; Scott, 1997), while low flow increases of 40 % to 1090 % have been measured in California and Washington, US and Alberta, CAN (Kinoshita and Hogue, 2015; Mahat et al., 2016; Niemeyer et al., 2020).

Shifts in the streamflow regime can have substantial impacts on aquatic ecosystems and downstream water supply. For example, elevated low flows, which are critical for aquatic ecosystem habitat, could help maintain cool stream temperatures and expand fish and other species' habitats during the critical summer months (Bradford and Heinonen, 2008; Mayer, 2012). Similarly, increased low flows could potentially provide additional water supplies to downstream communities during the summer period, which is often the period of highest water demand. Alternatively, post-fire increases in peak flow can lead to increased flooding and debris flow events (Moody and Ebel, 2012; Neary et al., 2003; Wall et al., 2020), increased water quality concerns like sediment, nutrients, and metals (Bladon et al., 2008; Emelko et al., 2016; Smith et al., 2011), and greater and more costly challenges for drinking water treatment (Emelko et al., 2011; Hohner et al., 2019).

However, there remains a lot of uncertainty about the post-fire hydrologic and water quality effects due to the substantial variability in responses as a result of site-specific controlling factors. For example, previous studies have identified burn severity (Rhoades et al., 2011; Rust et al., 2019), percent area burned (Rhoades et al., 2011), post-fire precipitation (Mast et al., 2016; Murphy et al., 2015), slope (Moody et al., 2013; Shakesby, 2011), aspect (Ebel, 2013), and aridity (Rust et al., 2019; Sheridan et al., 2015; Van der Sant et al., 2018) as potential controls on the streamflow or water quality response. However, little work has been done comparing the importance of these different factors to identify principal drivers, especially across scales from headwaters to downstream basin outlets. This type of information will facilitate improved policy and land management decisions to mitigate effects on source water supplies both before and after wildfires (Moody et al., 2013).

While previous studies have found increases in streamflow after wildfire, we have a poor understanding of the range of effects, particularly in larger basins (Emmerton et al., 2020; Hallema et al., 2017a; Shakesby, 2011; Wu et al., 2021). This is partially due to the random nature of wildfires, which makes tightly controlled experiments challenging. Thus, models provide an opportunity to make projections of the magnitude of effects and assess various post-fire scenarios. One of the major advantages of a modeling approach is its ability to simplify complex systems (Mirchi et al., 2010). This provides a cost- and time-effective way to generate high-frequency, continuous data (Borah and Bera, 2004; Lund and Palmer, 1997). Models also allow for standardized comparisons of future conditions and alternative scenarios (Borah and Bera, 2004; Lund and Palmer, 1997). Critics may argue that simplification renders model outputs of little value due to model assumptions and uncertainty and, indeed, some models should not be used to provide quantitative results. However, the reduced complexity makes models extremely useful for hypothesis development and testing, where those hypotheses can be field-tested in complex systems (Grayson et al., 1992). Additionally, for wildfire-specific studies, the ability of a model to provide unburned and burned outputs for the same spatial and climatic conditions overcomes one of the major challenges in wildfire research (Ebel and Mirus, 2014).

Several hydrologic models have previously been modified to investigate post-wildfire hydrologic responses (Ebel et al., 2023), including WEPP (Dobre et al., 2022), the McGuire-Rengers model (McGuire et al., 2017; Rengers et al., 2016), and the Soil and Water Assessment tool (SWAT) (Havel et al., 2018; Loiselle et al., 2020). However, many models, like WEPP, the McGuire-Rengers model, or RHESSys, are constrained to hillslope to small basin scales, and are rarely used to model wildfire effects at scales larger than 5 km^2 (Ebel et al., 2023). Comparatively, the SWAT model is a time-continuous, semi-distributed, process-based model that enables projections of streamflow at a river basin scale (Neitsch et al., 2011). Post-wildfire hydrologic modeling with SWAT has been completed for catchments in the Western US, Canada, Spain, Portugal, and Brazil (Basso et al., 2020; Loiselle et al., 2020; Morán-Tejeda et al., 2015; Rodrigues et al., 2019). These modeling efforts have projected increases in streamflow of 8 to >500 % at the subbasin scale (~5–270 km^2; Basso et al., 2020; Havel et al., 2018; Loiselle et al., 2020) and 2.4 % at the larger watershed scale (1500 km^2; Morán-Tejeda et al., 2015). Additionally, models have illustrated relationships between streamflow responses and both area burned (Havel et al., 2018; Rodrigues et al., 2019) and burn severity (Loiselle et al., 2020), which is consistent with empirical studies.

The objective of our study was to provide additional insights into the potential effects of large-scale wildfire on streamflow in two basins in the Pacific Northwest by using a modeling approach. Specifically, we sought to answer the following questions for key source water catchments on the west slopes of the Cascade Range in Oregon, US: (a) How does wildfire affect peak flows and annual water yields at the subbasin and basin scale? (b) How does watershed scale affect the magnitude of post-fire streamflow changes? (c) What are the principal drivers of differences in post-fire streamflow responses at the sub-catchment scale?

2. Materials and methods

2.1. Study area

Our study area included two large basins on the west slopes of the Cascade Range in Oregon, USA (Fig. 1). Specifically, we modeled the North Santiam River Basin (44°47′N, 122°45′W), which supplies

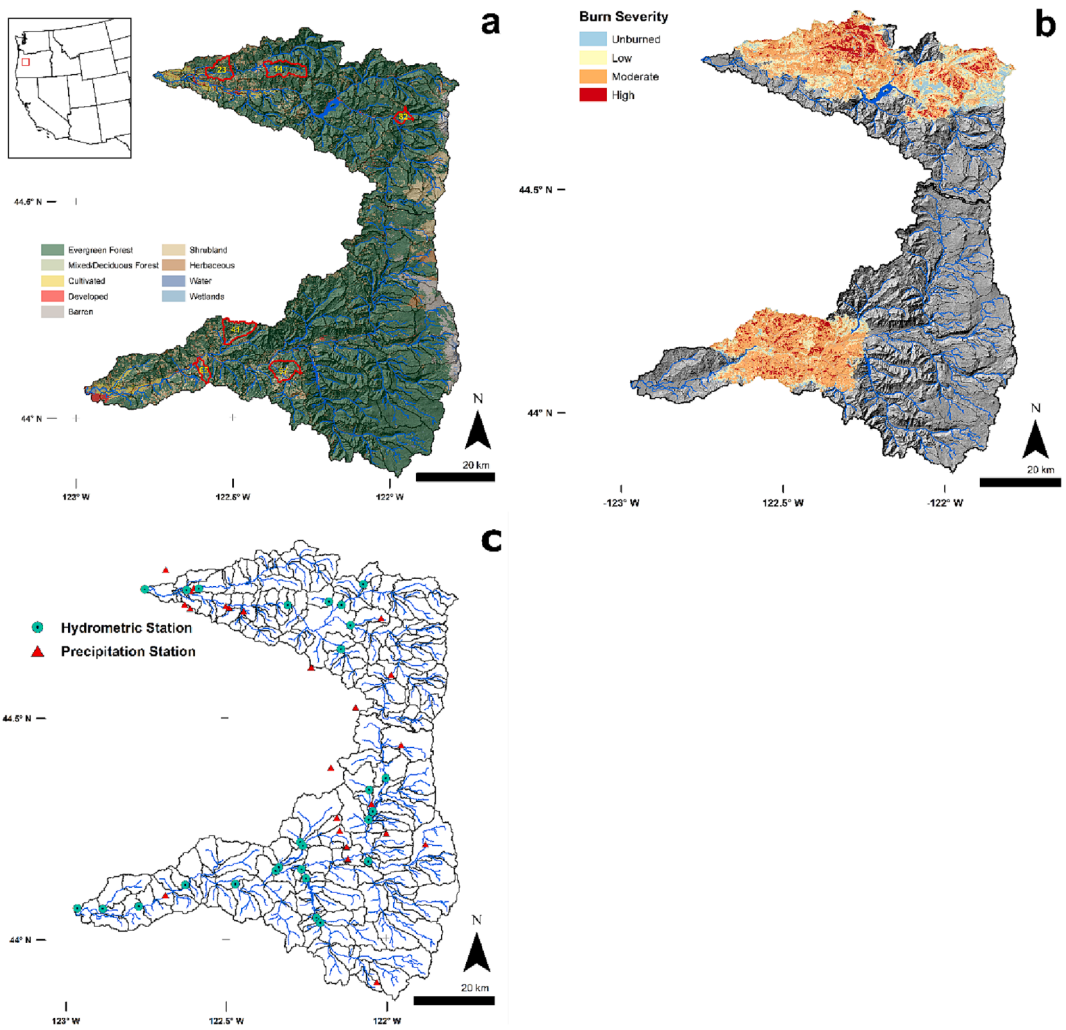

Fig. 1. (a) Map of land uses in the North Santiam (top) and McKenzie (bottom) basins in Western Oregon, USA. Important basins referenced in the results are labeled and outlined in red. (b) Map of the fire perimeters and soil burn severities for the Beachie Creek (top left) and Lionshead (top right) fires in the North Santiam basin and the Holiday Farm wildfire in the McKenzie basin, which burned in 2020 in Oregon, USA. (c) Locations of hydrometric and precipitation data used in the model calibrations.

drinking water to ~200,000 residents in the Salem, OR area. We also modeled the McKenzie River Basin (44°40′N, 122°57′W), which provides drinking water to ~200,000 residents in the Eugene, OR area. Both basins have steep, forested uplands where the headwaters to the North Santiam and McKenzie Rivers originate. Generally, both rivers flow west to agricultural land with little relief. Both basins are within a Mediterranean climate with cool, wet winters and dry, warm summers (Kottek et al., 2006; Snyder et al., 2002). The basins receive an average of 2,114 mm of precipitation annually—although, due to orographic effects, it ranges from approximately 1,000 mm to 3,000 mm (PRISM Climate Group, 2012). The basins are rain dominated below 400 m, mixed rain and snow between 400 and 1,200 m, and snow dominated above 1,200 m. The average annual water yield in the McKenzie at the Hayden Bridge treatment plant is 1,447 mm (2007–2019, USGS site 14164900). Average annual water yields in the North Santiam near the outlet are 1,830 mm (1960–2019, USGS site 14183000). Annual 30-year normal air temperatures range from minimums of −4.0–5.9 °C in the winter to maximums of 6.9–17.3 °C in the summer (PRISM Climate Group, 2012). Approximately 80 % of both basins are forested land, comprised mainly of Douglas-fir (*Pseudotsuga menziesii*), Western hemlock (*Tsuga heterophylla*), and Pacific silver fir (*Abies amabilis*). While our two study basins have many similarities, they also have slight differences in land use, geology, topography, and area (Table 1). Additionally, due to a large proportion of High Cascade geology, the McKenzie River Basin has many influential springs, which may contribute as much as 80 % of the discharge during the summer low flow period (Jefferson, 2006).

Wildfires in both basins have been relatively infrequent, with a total area burned from 1984 to 2019 of 14,746 ha in the North Santiam and 31,534 ha in the McKenzie. However, in August to October 2020, wildfires in the two basins burned a combined area of 146,580 ha, which was ~3.2-times greater than the total area burned from 1984 to 2019. Specifically, the Beachie Creek and Lionshead wildfires burned ~51 % of the North Santiam River Basin, with 67 % of the Beachie Creek fire and 45 % of the Lionshead fire burned at moderate to high severity (Table 2). Comparatively, the Holiday Farm fire burned ~18% of the McKenzie river basin at slightly higher severity with ~77 % of the area burning at moderate to high severity. As such, we sought to model the 2020 Oregon wildfires to provide insights into the potential range of streamflow responses and to identify dominant drivers of variability in post-fire streamflow.

2.2. Model description

To model the streamflow response to wildfire, we used the Soil and Water Assessment Tool (SWAT 2012, rev. 664). We chose the SWAT model because of its ability to simulate hillslope runoff processes,

Table 1
Characteristics of the study basins, the North Santiam and McKenzie, located in the Western Cascade Range in Oregon, USA.

	Study Watershed	
Parameter	N. Santiam	McKenzie
Major Land Uses	Forest-Evergreen (80%), Range-Brush (12%), Hay (1.7%), Range-Grasses (1.4%)	Forest-Evergreen (81%), Range-Brush (8.2%), Southwestern US (Arid) Range (3.6%) Range-Grasses (2.0%)
Land Ownership		
Public	70%	69%
Private	30%	31%
Geology		
Geologic Group	Little Butte Volcanics (30%), Quaternary surficial deposits (27%), Late Western Cascade Volcanics (18%), Late High Cascade Volcanics (17%)	Little Butte Volcanics (32%), Quaternary surficial deposits (23%), Late High Cascade Volcanics (21%), Late Western Cascade Volcanics (14%),
Primary Rock Type	Basalt (49%) and Sand (17%)	Basalt (66%) and Sand (15%)
Soils Textures	Silty Clay Loam, Clay Loam and Cobbly Loam	Silty Clay Loam, Clay Loam and Cobbly Loam
Elevation		
Minimum	45 m	89 m
Mean	899 m	974 m
Maximum	3170 m	3138 m
Max Slope	69.8°	74.2°
Mean Slope	16.2°	15.6°
Watershed Area (ha)	175,300	296,873

streamflow, and in-stream cycling of water quality parameters. SWAT is a physically-based, basin-scale, hydrologic model developed by the US Department of Agriculture. Basins are divided into sub-basins based on topographic maps and further divided into hydrologic response units (HRUs) based on land use, soil, and slope. Climate data is input into the model, which is used to calculate the water balance in each HRU, routing water, nutrients, and sediment through the basin (Gassman et al., 2007). SWAT was originally developed to model hydrology and crop growth in agricultural settings and has been modified to incorporate forested environments; however, the model does not have a built-in wildfire module. Thus, to simulate wildfire we modified individual parameters in the model source code (see section 2.4) to represent expected changes to the landscape and hydrology.

We constructed the models using the ArcSWAT (2012.10.5.21) interface with a digital elevation model (30 m resolution; U.S. Geological Survey, 2000), STATSGO2 soils data (30 m resolution; Natural Resources Conservation Service, 2006), and the 2016 National Land Cover Database (30 m resolution; Yang et al., 2018). We also used a 1/24 degree resolution downscaled global climate model for minimum and maximum daily air temperatures, average daily solar radiation, average daily wind speed, and average daily relative humidity from 1950 through 2019 (Abatzoglou and Brown, 2012). The best climate model for each variable was chosen by comparing the modeled climate variables to data from nearby meteorological stations (Table 3). Due to the importance of precipitation in modeling streamflow and the difficulty of modeling it at a daily scale, we used observed precipitation data from 1960 to 2019 from various publicly available sources (Daly et al., 2020; National Climatic Data Center, n.d.; Natural Resources Conservation Service Oregon, n.d.; The University of Utah, n.d.). We used data from 13 precipitation stations in the North Santiam basin and 21 precipitation stations in the McKenzie basin (Fig. 1). Precipitation was gap-filled using the *hyfo* package (Xu, 2020) in R.

In building the models, the basin outlet was set at the drinking water intakes for the cities of Salem (North Santiam) and Eugene (McKenzie). The Detroit Reservoir in the North Santiam Basin and the Blue River and Cougar Reservoirs in the McKenzie Basin were added into the model. This included setting up the reservoirs using the basin area and volume of both the emergency and principal spillways. We also input daily reservoir outflow data to the model to describe the daily outflow from each of the reservoirs (U.S. Army Corps of Engineers, n.d.). Model setup resulted in 125 subbasins (defined by SWAT as a first level subdivision of watersheds based on surface topography) in the North Santiam and 110 subbasins in the McKenzie Basin. The subbasins were then further divided into HRUs, where each HRU had a single slope class, soil type, and land use. As a compromise between data resolution and computational loads, we specified 15 % threshold values for slope, soil, and land use, where areas below those thresholds were dissolved into the existing slope classes, soil types, and land uses (Her et al., 2015). Any areas within each basin that were classified as water (i.e., SWAT model land use class "WATR") were retained as water in the model. This resulted in 1,112 HRUs for the North Santiam and 973 HRUs for the McKenzie Basin. Lastly, to account for inputs to streamflow from springs in the McKenzie, we included seven point sources for spring water discharge to subbasins using an average annual discharge of $>0.85\ m^3\ s^{-1}$, which was based on estimates by Jefferson et al. (2006).

2.3. Model calibration

For model calibration, we used the SWAT-CUP program (version 5.1.1) with the SUFI-2 method. Calibration was performed using a parallel processing program, allowing the simulations to run simultaneously on multiple cores, shortening the calibration process (Du et al., 2020). We used a warm-up period of four years and ran the model at a daily time step. Both models were calibrated for discharge from 2000 to 2019 using seven monitoring points in the North Santiam and 13 monitoring points in the McKenzie. Validation was performed from 1990 to 1999 using six monitoring points in the North Santiam and nine monitoring points in the McKenzie. Both models were calibrated for streamflow and sediment, while we only present streamflow results

Table 3
Climate models used in our SWAT simulations of the North Santiam and McKenzie River basins based on their correlation with observed meteorologic data.

Variable	North Santiam		McKenzie	
	Climate model	Mean R^2	Climate model	Mean R^2
Temperature	inmcm4	0.86	NorESM1-M	0.85
Relative humidity	MIROC-ESM-CHEM	0.41	MIROC-ESM-CHEM	0.41
Solar radiation	HadGEM2-CC365	0.86	HadGEM2-CC365	0.86
Wind speed	GFDL-ESM2M	0.15	GFDL-ESM2M	0.15

Table 2
Discovery date, area burned, and severity of the three wildfires that burned in the North Santiam and McKenzie Basins, Oregon, USA in 2020. Burn severity percentages were calculated from the severity classes identified in the BAER burn severity maps.

Wildfire	Watershed	Discovery date	Total area (ha)	Area in basin (ha)	Burn severity within basin			
					% unburned	% low	% moderate	% high
Lionshead	North Santiam	16 August 2020	82,794	38,448	15.9	39.0	35.0	10.0
Beachie Creek	North Santiam	16 August 2020	78,333	51,738	3.2	29.5	54.1	13.1
Holiday Farm	McKenzie	17 September 2020	70,169	56,394	3.8	20.8	65.6	11.0

here, calibrating for both streamflow and sediment increases confidence that the underlying physical processes are being correctly represented in the model. A regionalization approach was taken to calibrate the models, where calibration was performed for each subbasin with a monitoring point and its upstream basins. We first calibrated the upstream monitoring points, working downstream to the basin outlet. We evaluated model performance using the Nash Sutcliffe Efficiency (NSE) and adjusted R^2 coefficients (bR^2). Best parameters were determined by performing 500 simulations at a time, manually narrowing parameter ranges based on the best parameter values from the previous model run.

Observed discharge data used to calibrate the model was aggregated from several sources. The *waterData* package (Ryberg and Vecchia, 2017) in R (R Core Team, 2020) was used to obtain discharge data from USGS gauging sites. We also used stream discharge data from the HJ Andrews Experimental Forest (Johnson et al., 2020) and data on spring contributions to streamflow from Jefferson et al. (2006) to calibrate the model.

2.4. Wildfire simulations

We modeled both the Beachie Creek and Lionshead wildfires in the North Santiam Basin and the Holiday Farm wildfire in the McKenzie Basin. We set the start date of the wildfires in the model to 7 September 2020, which was the actual start date for the Holiday Farm fire and the date that the Beachie Creek and Lionshead fires rapidly expanded in size. A wildfire module was developed where, during a model run at the wildfire date, multiple parameters in the model were modified to represent the effects of wildfire on the landscape. To select the range of parameters to represent the effects of wildfire, we developed a conceptual model of expected effects based on literature values and expert opinion (Fig. 2). To model the mixed-severity burn patterns of the 2020 wildfires, we specified parameter changes for low, moderate, and high severity conditions. Wildfire severity was determined from severity maps created by U.S. Forest Service Burn Area Emergency Response (BAER) teams and used to assign burn severities to HRUs in the burned area. Specifically, we used the ArcMap "Zonal Statistics as Table" tool to calculate the mean burn severity for each HRU where burn severities were represented by increasing integer values. In our model, we ensured the percent area burned at each severity class matched the percent area burned at each severity class of the actual fire as closely as possible. To do that, we chose threshold values of the HRU averaged burn severity to classify HRU's with burn severities of low, moderate, and high. We used a broad definition of burn severity to refer to the effects of fire on the consumption of large fuels, shrubs, litter, organic matter, and buried plant parts (Monitoring Trends in Burn Severity, n.d.). Water HRUs were not burned in the simulation.

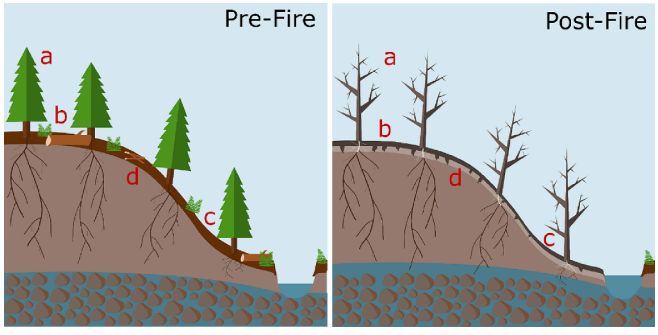

Fig. 2. A conceptual model showing the motivations behind the parameters modified within SWAT to simulate wildfire effects. Fire consumes vegetation, resulting in shifts in forest structure and decreasing transpiration (a). The loss of vegetation results in less ground cover and less surface "roughness" (b). Physical soil properties like bulk density and erosivity can be altered by the heat of the fire (c). Soil hydraulic properties like infiltration are often altered by wildfire, generally resulting in increased surface runoff (d).

We ran the calibrated models for one year following the fires, from 7 September 2020 to 6 September 2021. We chose to only simulate one year at a time due to annual model memory effects and because the model does not represent wildfire recovery. As such, running the model continuously in the post-fire period would not accurately represent continuous years of post-fire conditions. We repeated the model run 56 times for the McKenzie and 60 times for the North Santiam using different precipitation scenarios. Repeating the model run multiple times for the first post-fire year allowed us to hypothetically examine the effect of different annual precipitation in the initial post-fire period. Precipitation for each single year simulation was generated from the range of historical precipitation for each basin. During each simulation, a year of the precipitation data was selected from the historic record, matching the day of year (7 September 2020 to 6 September 2021), and used as the precipitation input for the post-fire year. For each simulation we used the reservoir data from the same year as the precipitation data to account for differing annual reservoir management. Other climate variables, including minimum and maximum temperature, wind speed, solar radiation, and relative humidity used the predicted values from the MACAv2 gridded climate model (RCP 8.5, Table 3) from 7 September 2020 to 6 September 2021. The historic precipitation data included years 1960–2019 from the North Santiam and 1964 to 2019 for the McKenzie.

We developed a module in SWAT to enable us to simulate the effects of wildfire by changing various model parameters such as saturated hydraulic conductivity, available water capacity, bulk density, soil and plant uptake evaporation compensation factors (used to adjust the depth distribution of soil and plant evaporative demand), curve number, Manning's *n* for overland flow, and land use type. Details on how each of these factors was modified to represent wildfire in the model are provided below and are summarized in Table 4.

2.4.1. Saturated hydraulic conductivity

Saturated hydraulic conductivity is used in the model to determine the rate of vertical water percolation through soil layers, it is not directly used to calculate runoff volumes. We modified soil saturated hydraulic conductivity in the upper soil layer based on the relationship developed by Moody et al. (2016) (Equation 1).

$$\boldsymbol{K_{fs}} = 2360\boldsymbol{e}^{-0.0056\boldsymbol{dNBR}} \quad (1)$$

where $\boldsymbol{K_{fs}}$ is field saturated hydraulic conductivity and dNBR is differenced normalized burn ratio, a satellite derived metric that is commonly used to capture wildfire-caused differences in leaf area, plant productivity, and moisture. For dNBR values less than 400 the saturated hydraulic conductivity remained unchanged. For calculating changes in saturated hydraulic conductivity using Equation (1), we selected dNBR values of <400 for low burn severity, 550 for moderate burn severity, and 800 for high burn severity based values proposed by Lutes et al. (2006). Since our starting, unburned saturated hydraulic conductivity values were different than those in Moody et al. (147 mm h^{-1}; 2016), we

Table 4
Summary of SWAT parameters modified in the wildfire module at each fire severity.

Parameter	Replacement type	Change based on fire severity		
		Low	Moderate	High
SOL_K(1)	relative	0%	−26%	−82%
SOL_AWC	relative	−25%	−70%	−90%
SOL_BD(1)	relative	1%	9%	13%
ESCO	replace	0.5	0.8	1
EPCO	replace	0.5	0.2	0.01
OV_N	replace	0.8	0.4	0.011
Land Use	replace	FRSE	RNGE	BARR
CN2	additive	10	20	30

quantified the absolute change between their starting values and the values predicted by the dNBR thresholds. We then converted those values to a relative change, which was broadly applicable across saturated hydraulic conductivities. This resulted in modifications of hydraulic conductivity of 0 % for low severity, −26 % for moderate severity, and −82 % for high burn severity for the fire module.

2.4.2. Available water capacity

During calibration we increased the available water capacity—a model parameter to account for the water available to plants for transpiration—in the soils to account for the high resistance to xylem dysfunction and ability to transpire at low soil water potential by Douglas-fir, the dominant tree species in our study basins (Brooks et al., 2006; Domec et al., 2008, 2004; Fan et al., 2017). However, for the wildfire scenario, we decreased the available water capacity to account for post-fire changes in vegetation (i.e., mortality of Douglas-fir trees due to wildfire) to help meet the expected decrease in catchment-level transpiration, which has been observed to decline by up to ~55% following high severity wildfire (Ma et al., 2020; Roche et al., 2018). Available water capacity was reduced 90 % for high severity, 70 % for moderate severity, and 25 % for low severity. Available water capacity changes were determined by testing scenarios where the entire basin burned and choosing changes that would result in ET drops matching existing literature values (Ma et al., 2020; Roche et al., 2018). Admittedly, adjusting available water capacity is not an ideal way to account for decreased transpiration post-fire, as it can impact the amount of water held within the soil. Leaf area index and rooting depth also control plant transpiration within the model. However, we found these parameters insensitive. Which is likely due to SWAT's origins as an agricultural model, as such, forests are typically not well represented (Haas et al., 2022).

2.4.3. Soil bulk density

We increased the bulk density of the upper soil layer by 13 % for high severity, 9 % for moderate severity, and 1 % for low severity fire. We determined these estimates of post-fire changes in bulk density from literature values associated with laboratory burning experiments (Badía and Martí, 2003; Stoof et al., 2010) and empirical studies (Ebel and Moody, 2020; Xue et al., 2014). In general, the heat generated during wildfires can affect soil texture (Badía and Martí, 2003; Ulery and Graham, 1993), organic matter content (Alauzis et al., 2004; García-Corona et al., 2004), and overall soil structure (Ebel and Moody, 2020), which modify the overall bulk density.

2.4.4. Soil and plant uptake evaporation compensation factors

The soil evaporation compensation factor (ESCO) is a coefficient in the model that allows the user to modify the depth distribution of soil evaporation. The coefficient ranges from 0.01 to 1.0, as ESCO decreases, more water can be taken from deeper soil levels. Similarly, the plant uptake compensation factor (EPCO) is a coefficient that allows the user to modify the depth of water in the soil that vegetation can access for transpiration, EPCO also ranges from 0.01 to 1.0, however in this case, larger values equate to water demand able to be met by deeper soil levels. In our wildfire scenarios, we increased the ESCO and decreased the EPCO, which limited the depth of soil water use after fire occurrence. Specifically, for high severity, we set ESCO to 1 and EPCO to 0.01, for moderate severity we set ESCO to 0.8 and EPCO to 0.2, and for low severity we set ESCO and EPCO to 0.5. These modifications were made based on the loss of overstory vegetation and transpiration due to wildfire, as well as the increased bulk density (Ebel and Moody, 2020; Xue et al., 2014), surface sealing (Larsen et al., 2009), water repellent layers (Nyman et al., 2010; Robichaud, 2000), and a loss of porosity (Xue et al., 2014), which can all contribute to more surficial evaporative processes.

2.4.5. Curve number

The curve number is a widely used parameter for projecting the approximate proportion of precipitation that ends up as direct runoff. We increased the curve number relative to the initial values associated with the soils by 10 units for low severity, 20 units for moderate severity, and 30 units for high severity burns. If these increases resulted in a curve number greater than 98, we adjusted the values back to a maximum of 98, which was representative of impervious surfaces. We determined these shifts in curve number values based on knowledge that changes in soil physical properties due to wildfire can lead to elevated infiltration excess overland flow (Malvar et al., 2011; Onda et al., 2008) and was consistent with previously proposed adjustments (USDA, 2013; USDA Forest Service, n.d.).

2.4.6. Manning's "n" for overland flow

We also changed the Manning's n values—a hydraulic roughness coefficient—to account for the differential effects of wildfire severity on soil surface roughness and resistance to overland flow. In general, greater wildfire severity results in greater ground cover consumption and loss of surface roughness components (Keeley, 2009; Parson et al., 2010). Thus, we related the expected remaining ground cover associated with different burn severities to similar Manning's n ground cover values. Specifically, we set Manning's n to 0.80 for low severity, 0.40 for moderate severity, and 0.011 for high severity fires, which was also consistent with previous studies (USDA Soil Conservation Service, 1986).

2.4.7. Land use

Given that wildfires can dramatically change forest structure and composition (Halofsky et al., 2020; Meng et al., 2015), we used the land use function in the model to represent the expected shifts in forest ecosystems associated with different fire severities. We made this decision because there was no option in the model to modify forest density but required a way to model the post-fire effects on the loss of evapotranspiration. Similar land use changes have been used previously within SWAT to account for post-fire decreases in transpiration (Loiselle et al., 2020). As such, we updated the land use, focusing principally on the loss of woody biomass from trees. Specifically, for low severity burns we did not change the original land use and, as such, forested areas were still considered to be forested as evergreen or conifer forests (FRSE). For moderate severity burns, we changed the land use to grasses (RNGE) while for high severity burns, we updated the land use to barren (BARR). These changes were necessary to produce a reasonably realistic reflection of the transpiration loss associated with wildfire, which is often the dominant hydrological process that is impacted, leading to additional water availability for runoff generation and streamflow (Ma et al., 2020; Niemeyer et al., 2020).

2.5. Sensitivity analysis

To determine the most sensitive parameters in our wildfire model, we ran a sensitivity analysis for both the North Santiam and McKenzie models. For each model we ran three wildfire scenarios, a low, moderate, and high where the entire basin was burned at that severity. Sensitivity was tested by varying the parameters used in the wildfire module one at a time, running 100 simulations for each parameter with values ranging from the low to high severity wildfire module values. To test land use change, we replaced the existing land cover with the other generic land cover types one at a time, excluding water, which was a total of 18 simulations. For each scenario, initial conditions were set to the burned, wildfire module values for that severity, and a median precipitation scenario was used. Sensitivity was determined for both annual water yields and peak flows by first calculating the average change from the base, unburned scenario across all subbasins in the model. Then to get a measure of sensitivity we calculated the standard deviation of the average change across both models.

2.6. Statistical analysis

Unfortunately, model predictions of streamflow often remain inaccurate with substantial uncertainty due to limited calibration data, unresolved model parameter values, and poor representation of physical processes (Faramarzi et al., 2015; Zaremehrjardy et al., 2021). However, in our study, we were not concerned about producing accurate predictions of the streamflow response to wildfire. Rather, we were interested in quantifying and estimating the relative change in streamflow from the unburned to burned scenarios, which enabled us to not be constrained by model uncertainty. Model calibration ensured that the physical processes were reasonably represented—our model fits provided evidence that the model was indeed representing the physical processes adequately. Despite the adequate representations of physical processes in the model, differences in model parameterization can produce variability in relative streamflow changes (Boisrame et al., 2019).

Annual summaries of water yield and peak streamflow were determined for both the basin outlets and the headwater subbasins, where the headwater subbasins did not have upstream subbasins. Peak streamflow was determined as the maximum daily flow in each precipitation scenario year. Linear mixed effects (LME) models were created for annual water yields and peak streamflow using the *nlme* package in R (Pinheiro et al., 2020). This analysis was used to find the differences between burn and unburned scenarios and test if there was statistical evidence for an effect of wildfire. The basin and wildfire scenario were the fixed effects in the model with precipitation scenario/basin as nested random effects. Variance of errors were allowed to vary by basin. Subbasins that were not burned were removed before analysis. Additionally, to simplify the headwater models, we used the mean percent change of all the headwater subbasins in each model for each precipitation scenario. The LME model for peak streamflow changes at the headwater scale was $\log_{10}$ transformed to normalize the residuals. We used the R package *emmeans* to extract the mean and 95 % confidence intervals from the LME model and ran Tukey multiple comparison tests to check for significant difference in the mean values between groups (Lenth, 2021).

To visualize the effect of the wildfire scenario across all flow magnitudes, flow duration curves were created for both the burned and unburned scenarios for individual subbasins. The streamflow data was sorted and ranked by descending magnitude, including all the precipitation scenarios. Similarly, flood recurrence intervals for both burned and unburned scenarios were calculated by ranking the streamflow across all precipitation scenarios in descending order of magnitude. We then calculated return periods and probabilities using the Weibull plotting position method (Helsel et al., 2020).

We also performed random forest analyses to identify variables of importance (i.e., burn severity, land-use, aspect, geology; Table A2) in driving post-fire streamflow changes. We performed two separate analyses, one for annual water yield and one for peak streamflow changes. We combined the data for both basins for each analysis. The explanatory variables came from GIS data layers, which were aggregated to a subbasin level using the ArcMap "Zonal Statistics as Table" tool to calculate the mean (for continuous data) or mode (for categorical data). Then we linked the streamflow data to the aggregated landscape and climate variables associated with each subbasin (Table A2). To numerically compare the burn severity across subbasins for the random forest analysis, a metric of relative burn severity was developed by averaging the wildfire pixels in the area of each subbasin, where 0 was unburned, 1 was low severity, 2 was moderate severity, and 3 was high severity. Thus, the metric ranged from 0 to 3, with increasing values representing higher severities.

The random forest analysis was performed using the 'cforest' function in the *Party* package in R (Hothorn et al., 2006; Strobl et al., 2008, 2007) for both percent change in annual streamflow and percent change in maximum annual peak flow. Variable importance was determined using the permutation method to find the mean decrease in accuracy of the random forest model on the out-of-box data using the 'varimp' function. Analysis used 2000 trees, 'mtry' was set to 9, and the model did not use replacement when sampling the observations, as recommended by Strobel et al. (2007) for accurate variable importance measures. The subbasins upstream of the fire were removed for analysis. Due to the limited number of data points, the entire dataset was used for training. Model fit was determined using the out of box data to calculate a pseudo R^2 value by using the 'predict' function from the *Party* package to calculate the sum of squares residuals. To investigate directionality of the driver variables, partial dependence plots were found for the five most important variables in each model using the *pdp* package in R (Greenwell, 2017). To minimize computational time, 15 equally spaced points were used for continuous variable plots. A second set of random forest models were created to look at mean burn severity in each subbasin based on the real burn severity wildfire maps. These models used the same procedure to the other models except in the burn severity random forest all the subbasins were retained in the analysis.

3. Results

3.1. Calibration

The daily streamflow calibration for the North Santiam model had a mean Nash Sutcliffe efficiency coefficient (NSE) of 0.48 ± 0.19. This was slightly better than the streamflow calibration for the McKenzie Basin, which had a mean coefficient value of 0.40 ± 0.47 (Fig. 3). In the validation period, the North Santiam had a mean NSE of 0.35 ± 0.32 while the McKenzie had a mean coefficient value of 0.56 ± 0.19 (Fig. 3). Although previous recommendations for modeling daily streamflow data have indicated a NSE above 0.50 as satisfactory and above 0.70 as good (Moriasi et al., 2015), these recommendations are principally for small, headwater catchment scale studies. Such studies typically only include a single basin at the outlet; however, our models included 6 to 13 calibration points in each basin, making it challenging to achieve an overall NSE value above 0.7. Given the complexity of our study basins, we found these model fits satisfactory. See Table A1 for more detailed calibration results.

3.2. Validation of wildfire module

We validated our model outputs for the wildfire simulations by comparing predicted streamflow values with a year of observed streamflow from USGS gauges following the wildfires, using the most severely burned sub-catchment in each basin which had measured streamflow data available. We validated the outputs in the North Santiam Basin with data from subbasin 23, which had a burn severity of 1.86 out of 3—a moderate to high burn severity sub-catchment. The observed annual water yield for the first year post-fire was 2,085 mm. Comparatively, the average predicted annual water yields were 1,449 ± 448 mm for the unburned scenarios and 1,644 ± 462 mm for the burned scenarios. While the model underestimated the actual annual water yield, the annual water yields (1960–2019) in the burned scenario were more similar to the observed data than the unburned scenario (Fig. 4). The average observed low flows (June through August) were 0.77 ± 0.54 mm d^{-1}, while average low flows were 0.46 ± 0.30 mm d^{-1} for the unburned scenarios and 0.79 ± 0.48 mm d^{-1} for the burned scenarios. The observed peak flow for the first year post-fire, 103.2 mm d^{-1} exceeded both model predictions. The mean predicted peak flow was 34.6 ± 15.8 mm d^{-1} for the unburned scenarios and 50.4 ± 20.2 mm d^{-1} for the burned scenarios.

Comparatively, in the McKenzie, subbasin 65 had a relative burn severity of 0.35 out of 3, so it was less fire-affected overall. This was reflected in the smaller differences between the unburned and burned scenarios (Fig. 4). The observed annual water yield in the first post-fire year was 1,279 mm. This was slightly lower than our modeled annual water yield (1964–2019) of 1,313 ± 246 mm in the unburned scenario and 1,342 ± 248 mm in the burned scenario. Similarly, observed

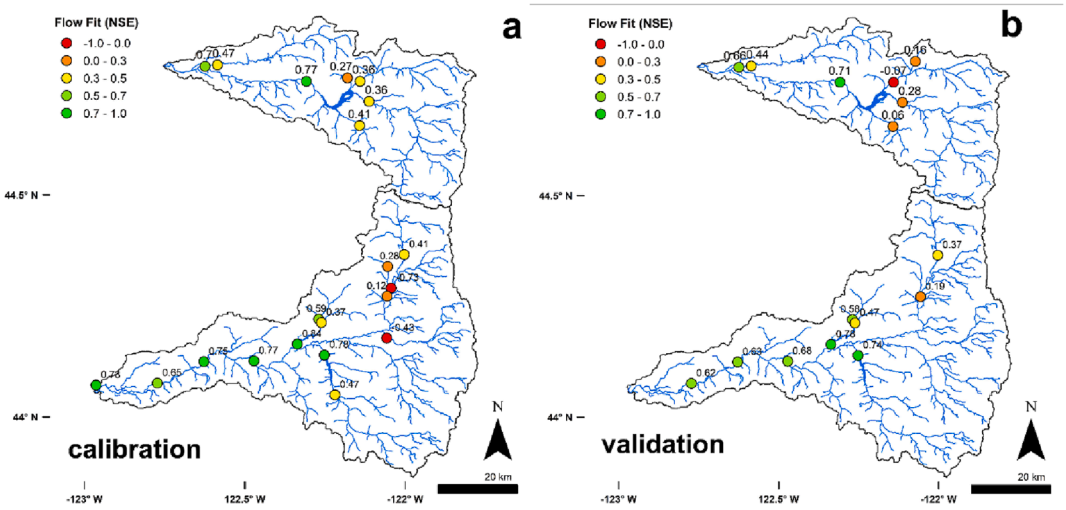

Fig. 3. The location and fit of the (a) calibration data (2000 to 2019) and (b) validation data (1990 to 1999) for the North Santiam (upper) and McKenzie (lower) River basins. Each dot represents a location where we calibrated streamflow with the color and value representing the goodness of fit using the Nash Sutcliffe Efficiency Coefficient (NSE).

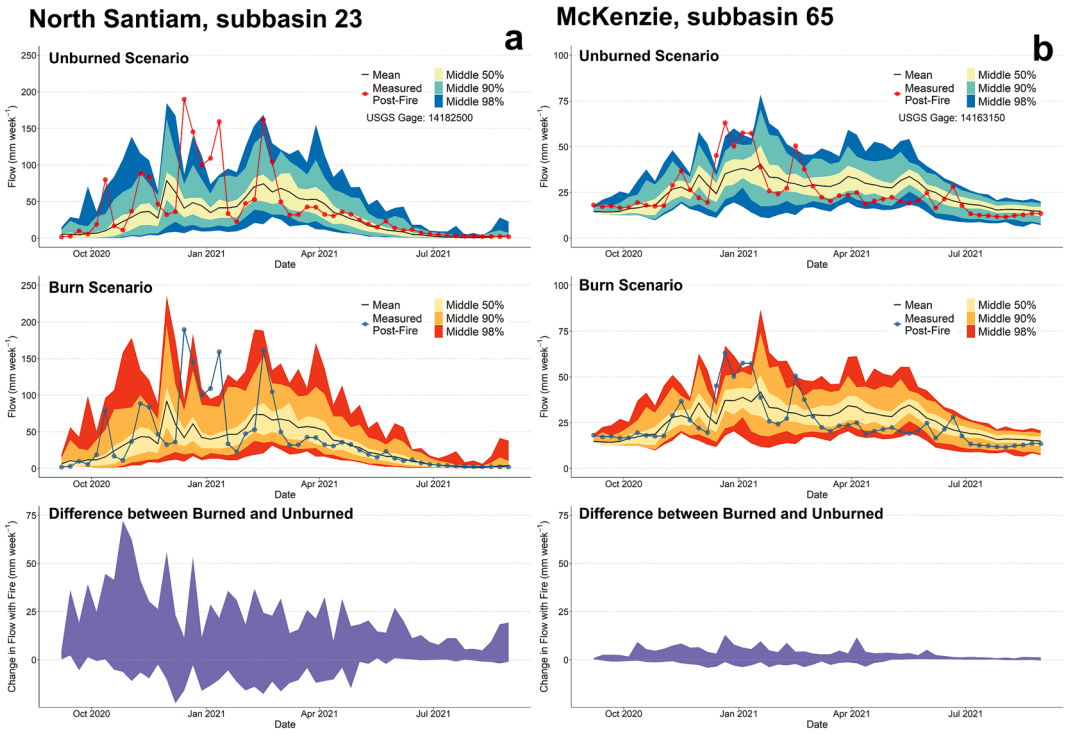

Fig. 4. (a) Measured streamflow (USGS Gage 14182500) compared with the model results the same location (Subbasin 23) in the North Santiam for the unburned and burned scenarios. (b) Measured streamflow (USGS Gage 141631150) compared with the model results the same location (Subbasin 65) in the McKenzie for the unburned and burned scenarios. The colored bands represent the 50, 90, and 98th percentiles of model outputs of streamflow from the range of inputs of precipitation scenarios. The bottom panel shows the difference between the burned and unburned scenarios where the ribbon is bounded by the minimum and maximum change in streamflow for every week.

average low flows (June through August) were slightly lower than both modeled scenarios. The observed mean low flows were 2.28 ± 0.81 mm d^{-1} while the unburned scenarios had a mean of 2.66 ± 0.57 mm d^{-1}, and the burned scenarios had a mean of 2.74 ± 0.59 mm d^{-1}. Peak flows, however, were better represented by the burned scenario. The peak flow for the observed data was 13.6 mm d^{-1} while the mean modeled peak flows were 10.1 ± 3.2 mm d^{-1} for the unburned scenarios and 12.5 ± 4.4 mm d^{-1} for the burned scenarios.

3.3. Magnitude and range of wildfire effects

Inclusion of the wildfire simulations in our models increased annual water yields in the North Santiam by an average of 14.6 % at the headwater scale and 8.0 % at the basin outlet scale.

Comparatively, the wildfire simulations in the McKenzie Basin increased annual water yields on average by 10.5 % in the headwater sub-catchments and 2.2 % at the basin outlet (Table 5). While the wildfire simulations resulted in modest increases in annual water yields, there were much larger increases in peak streamflow. In the North

Table 5
Effects of wildfire on annual water yields and peak flows at different spatial scales for the North Santiam and McKenzie River Basins, Oregon. Significance of the effect of wildfire was determined using the Tukey multiple comparisons test with our linear mixed effects models.

Streamflow parameter	Scale	Basin	Scenario	Mean	95% confidence interval		Wildfire effect		Basin wildfire effect	
					Lower	Upper	*t*-value	*p*-value	*F*-value	*p*-value
Annual water yield (mm year^{-1})	Headwaters	McKenzie	Unburned	986	896	1077	40.9	<0.001	519	<0.001
			Burned	1090	1000	1180				
		N Santiam	Unburned	1287	1197	1376	68.7	<0.001		
			Burned	1475	1386	1565				
	Outlet	McKenzie	Unburned	1251	1185	1317	39.8	<0.001	1776	<0.001
			Burned	1278	1212	1344				
		N Santiam	Unburned	1167	1101	1232	65.4	<0.001		
			Burned	1261	1195	1326				
Peak flow (mm day^{-1})	Headwaters*	McKenzie	Unburned	16.3	14.7	18.2	42.9	<0.001	124	<0.001
			Burned	31.8	28.6	35.4				
		N Santiam	Unburned	25.5	23.0	28.3	48.6	<0.001		
			Burned	40.5	36.5	44.9				
	Outlet	McKenzie	Unburned	9.69	8.61	10.8	11.6	<0.001	0.061	0.806
			Burned	12.1	11.0	13.2				
		N Santiam	Unburned	13.1	12.0	14.1	10.0	<0.001		
			Burned	15.4	14.4	16.5				

Note. Wildfire Effect tests the difference in means between the unburned and burned scenarios. Basin-Wildfire Effect tests if there is an interaction between basin and wildfire, answering do the basins have different responses to fire. *Peak flows for the headwater were $\log_{10}$ transformed, so the mean shown is the geometric mean.

Santiam, peak streamflow was increased an average of 58.8 % in the headwater sub-catchments and 17.6 % at the basin outlet. In the McKenzie, the geometric mean of peak flows increased 95.0 % in the headwater sub-catchments and increased 24.9 % at the basin outlet. Statistically, from our linear mixed effects models, there was strong evidence ($p < 0.001$) that the wildfire simulation increased both the mean annual water yield and peak streamflow in both basins (Table 5). There was also strong evidence ($p < 0.001$) that there was an interaction effect between basin and wildfire for mean annual water yields at both scales and peak streamflow at the headwater scales, meaning that the

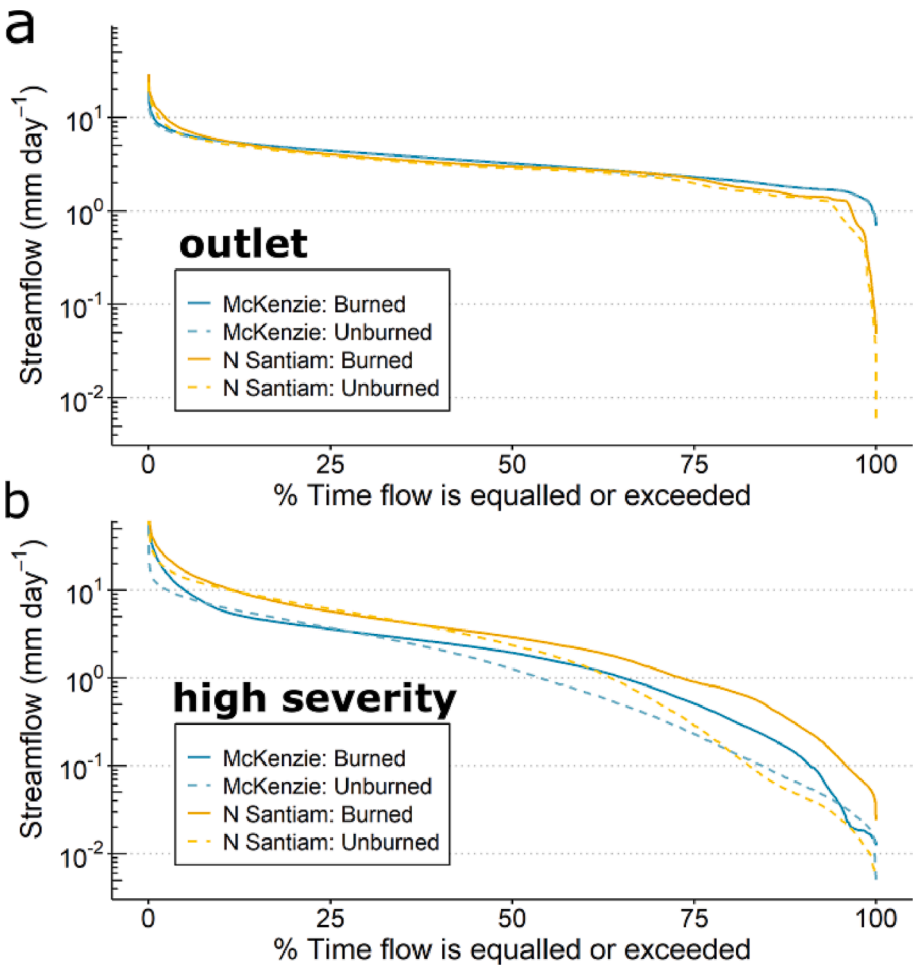

Fig. 5. Flow duration curves in the McKenzie and North Santiam, Oregon at (a) the basin outlet and (b) for two selected high severity subbasins, 41 in the McKenzie and 14 in the North Santiam. The burned scenario is shown as a solid line and the unburned scenario as a dashed line.

effect of wildfire was different between basins. Similarly, the flow duration curves for each of the study basins, illustrated an increase in the infrequent, high flows, or the largest 5% of flows (Fig. 5). For example, the largest 5% of flows in the severely burned headwater catchments of the North Santiam increased by 37.0 %. Interestingly, the largest 5% of flows in the severely burned headwater catchments in the McKenzie Basin increased by 128 %. At the larger basin scale, the upper 5% of flows at the North Santiam Basin outlet increased 17.0 %, while in the McKenzie Basin they increased by 29.5 %. Flood recurrence intervals also showed increased high flows. For example, at the North Santiam Basin outlet, the streamflow for a 1-year flood was increased 12.5 % and the ~6-year flood was increased 20.0 %. At the McKenzie Basin outlet there was a 10.8 % increase in streamflow for the 1-year flood and 25.8 % increase in the ~6-year flood. While these changes at the basin scale were notable, there were much larger increases in the magnitude of 1- and 6-year floods in the headwater sub-catchments that were burned at high severity (Fig. 6). For example, in the North Santiam in subbasin 14, the 1-year flood was increased by 45.5 % while the ~6-year flood was increased by 37.8 %. In subbasin 41 in the McKenzie, the 1-year flood was increased by 146 % while the ~6-year flood was increased by 156 %.

The flow duration curves from both basins, also illustrated that the burn scenario resulted in increases in summer low flows (Fig. 5). For example, in a severely burned subbasin in the North Santiam, the lowest 5% of flows increased from 0 mm d^{-1} to 0.025 mm d^{-1}, while the lowest 5% of flows in a severely burned basin in the McKenzie increased by 144 %. At the basin outlet of the North Santiam, the lowest 5% of flows increased by 179 %. However, at the outlet of the McKenzie Basin, the lowest 5% of flows increased by only 0.43 %. Overall, the effect of wildfire on annual water yields, peak flows, and low flows was most evident in headwater catchments and was dampened at the outlet of both basins (Fig. 7).

3.4. Drivers of post-fire streamflow changes

Our random forest model for annual water yields (pseudo $R^2 = 0.89$; Fig. 8) indicated that burn severity was the most important variable for describing changes between the unburned and burned scenarios, accounting for 52.4 % of model accuracy. Our model also indicated that annual precipitation was the second most important variable influencing annual water yields, representing 16.7% of the model accuracy. Percent area burned was the third most important variable influencing annual water yields, accounting for 13.4 % of the model accuracy. Other important variables for annual water yield changes included vegetation type and aridity which accounted for 5.4 % of model accuracy. The remaining variables accounting for the last 12 % of the model accuracy.

Our random forest analysis for peak flow changes found different driving factors than the analysis for annual water yields (pseudo $R^2 = 0.80$; Fig. 8). Here, the wildfire characteristics, burn severity and percent area burned, were the most important variables. Burn severity accounted for 39.0 % of model accuracy with percent area burned accounting for 21.7 %. Other important variables for peak streamflow changes included aridity, soil type, and geologic province, which were responsible for 20.7 % of model accuracy. The remaining variables accounted

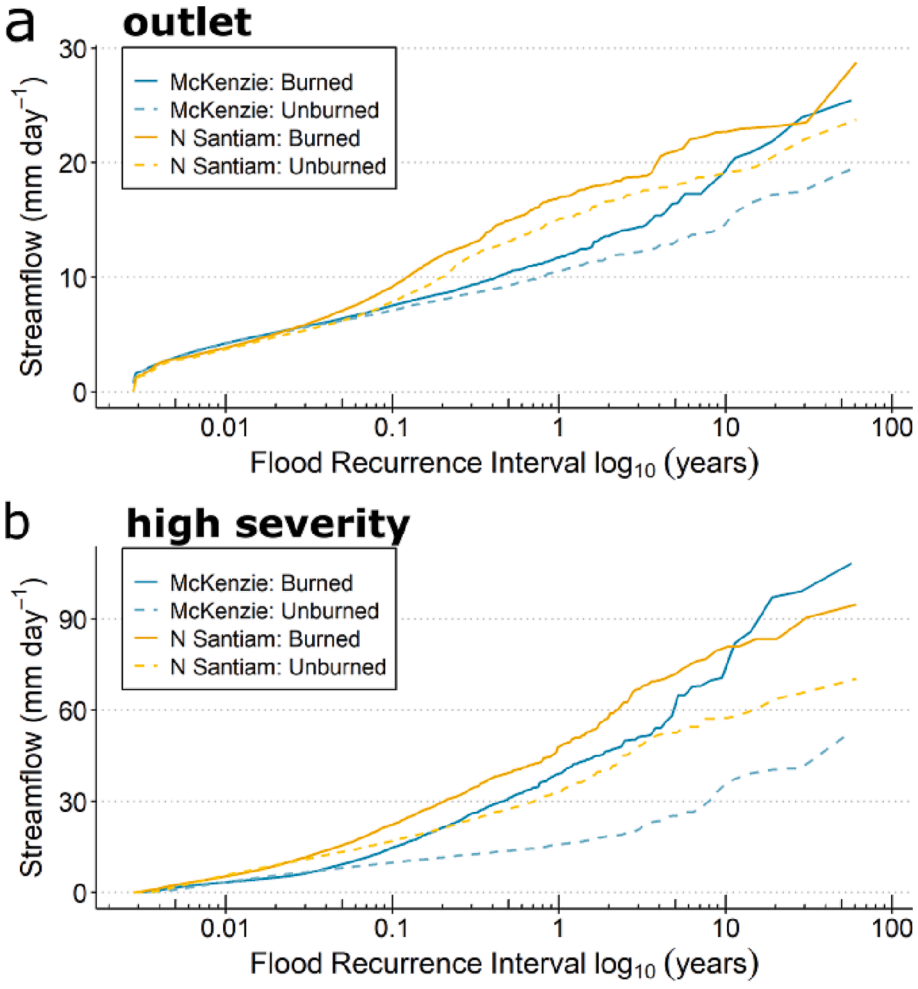

Fig. 6. Flood recurrence intervals at the outlet (a) and two severely burned subbasins (b) subbasin 41 in the McKenzie and 14 in the North Santiam, Oregon for the burned and unburned scenarios.

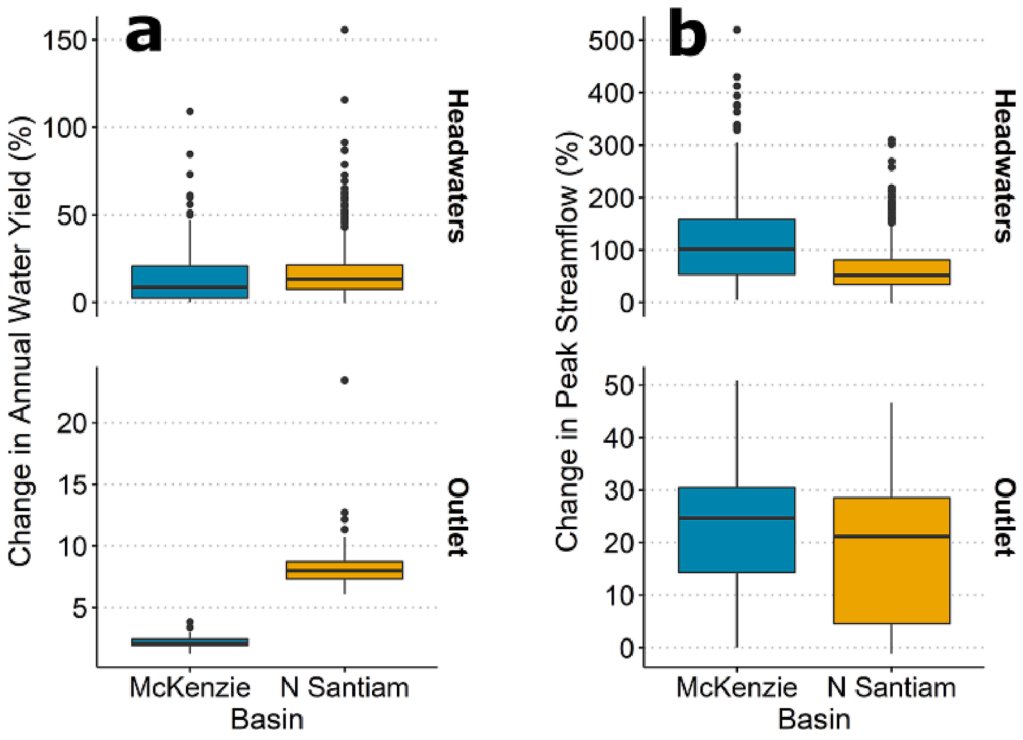

Fig. 7. Percent change between the unburned and burned scenarios for (a) annual water yield and (b) peak flows at the outlet and headwater scales for the McKenzie and North Santiam basins, Oregon. Data presented is across all the subbasins and all the precipitation scenarios.

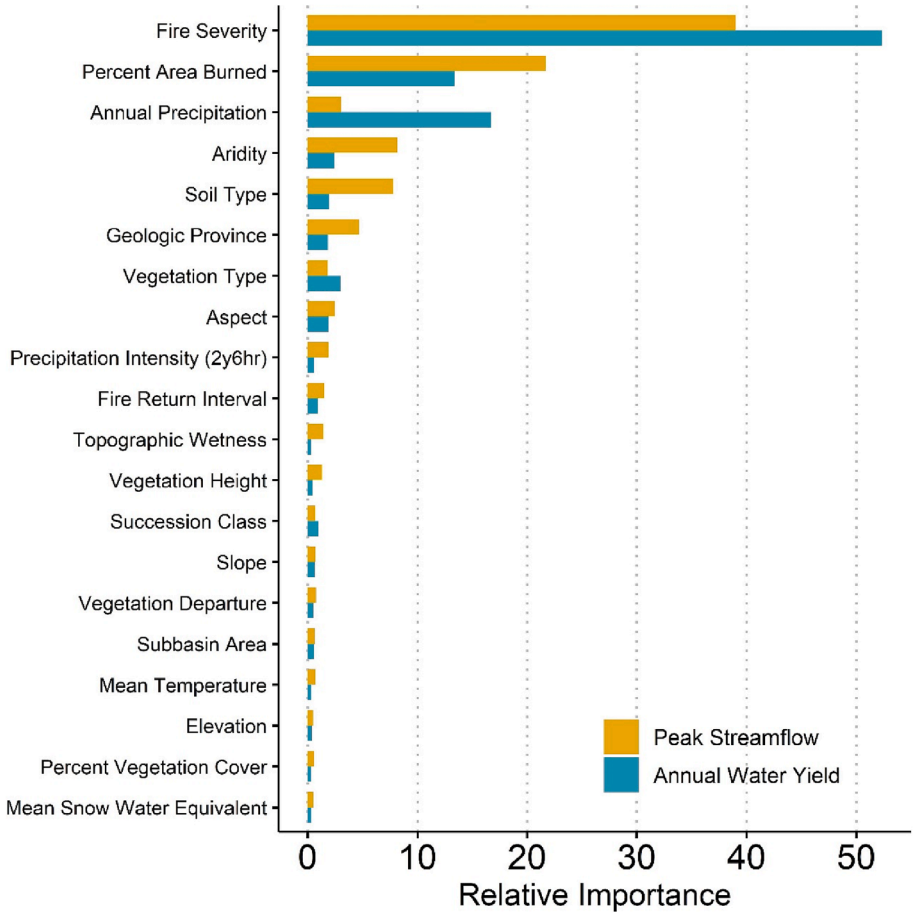

Fig. 8. Relative importance of factors used to determine the change between unburned and burned scenarios in peak flows (yellow) and annual water yields (blue) in the North Santiam and McKenzie basins, Oregon determined by random forest analysis.

for the last 18.6 % of model accuracy.

4. Discussion

As expected, the results from our model indicated that burn severity and percent area burned were generally the most important factors for projecting both peak flow and annual water yield changes after wildfire in the McKenzie and North Santiam basins, Oregon (Fig. 8). This finding is consistent with previous models, which indicated that burn severity or area burned are key predictors of post-fire peak flow responses (Kinoshita et al., 2014) or annual water yields (Feikema et al., 2013). Several empirical studies have also illustrated the importance of burn severity or the proportion of catchment area burned for driving the streamflow response. For example, both burn severity and percent area burned were positively correlated with increased peak flows, low flows, and runoff ratios from 82 burned watersheds in the western US (Saxe et al., 2018). Similarly, changes in annual streamflow were related to high burn severity in 25 catchments in the Pacific Northwest using five years of both pre-fire and post-fire data (Hallema et al., 2017a). Elevated streamflow after wildfires is often attributed to decreased evapotranspiration and changes to soil hydraulic properties, resulting in a greater proportion of precipitation ending up in streams (Ebel et al., 2012; Ma et al., 2020; Moody et al., 2016, 2008). For instance, seven watersheds in New Mexico exhibited elevated post-fire runoff ratios in areas where hillslope flow paths were burned at high severity (Moody et al., 2008). However, while many studies have found a linkage between burn severity and percent area burned and the resulting hydrologic response, wildfire effects have been highly variable and are likely due to catchment differences in geophysical properties and climate (Kinoshita et al., 2014; Saxe et al., 2018). Better understanding of how these differences affect post-fire streamflow changes is key to identifying areas vulnerable to post-fire effects, which will help inform land management decisions both before and after fire.

Indeed, the proportional changes in annual water yield due to wildfire in our two study basins were also related to catchment characteristics and climatic variables. Specifically, annual precipitation was the second most important variable in our random forest analysis for describing the change in annual water yield. The largest annual water yield gains generally occurred during wet years (Fig. A1). However, drier years had greater percent changes in annual water yields between the burned and unburned scenarios compared to wetter years (Fig. 9). We posit this was likely due to a greater proportion of the gross precipitation allocated to evapotranspiration (ET) in the unburned scenario for drier years. Several empirical studies have also identified precipitation as an important driver of post-fire annual water yields. For example, when post-fire streamflow was separated using climate elasticity models

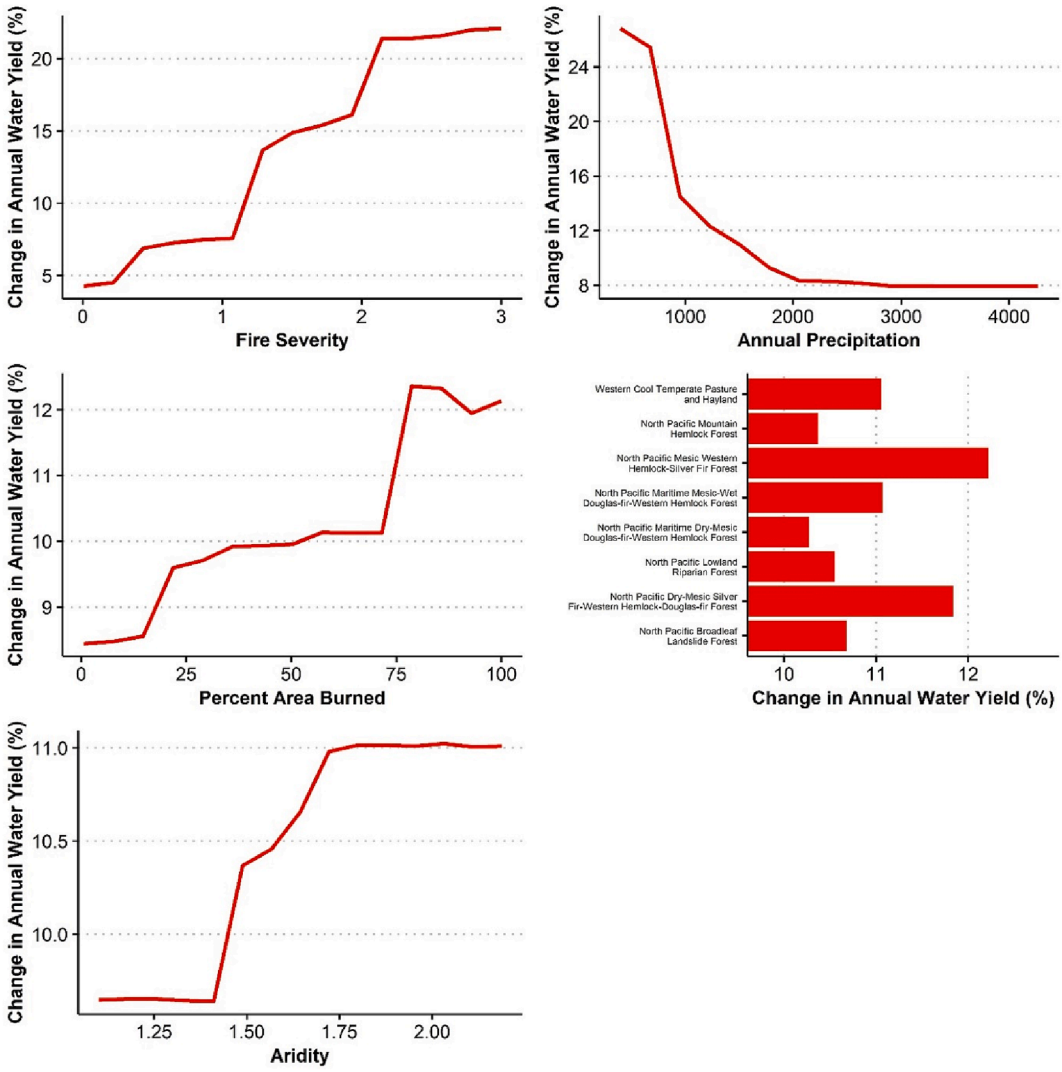

Fig. 9. Partial dependence plots for the five most important variables from the annual water yield random forest model for the North Santiam and McKenzie basins, Oregon. Plots show the relationship between the variable and relative annual water yield change between the burned and unburned scenarios.

for a burned watershed in California, streamflow was reduced 102 % due to precipitation but increased 38 % due to fire (Hallema et al., 2017b). Similarly, annual water yields increased after wildfire in six paired catchments in California, especially in years with average or above average precipitation (Bart and Hope, 2010). A review of 162 large watersheds that experienced land-use changes also indicated that watersheds receiving less annual precipitation were more sensitive to water yield changes after the disturbance (Li et al., 2017).

While fire characteristics and annual precipitation were the primary drivers of post-fire annual water yields—explaining 82 % of the variation in annual water yield changes—the random forest model also identified vegetation type and aridity as important variables (Fig. 8). Specifically, partial dependence plots indicated greater changes in annual water yields after fire in less arid areas and in catchments dominated by Pacific silver fir trees (Fig. 9). This was expected as these areas tended to have greater rates of ET during the pre-fire period. After wildfire, these areas likely experienced greater decreases in ET due to vegetation loss, leading to greater post-fire changes in runoff and streamflow. This is consistent with a post-fire study in California, where higher density forests had larger changes in post-fire ET, with the greatest decreases occurring in evergreen forests compared to other land use types (Ma et al., 2020). A number of general land use studies have also found that catchments draining conifer forests exhibited the greatest increases in water yields after disturbance. For example, a paired watershed study from the Pacific Northwest and Eastern US examined streamflow changes following harvesting during the wet, moist season; they found the greatest increases in streamflow occurred in hemlock forests followed by mixed conifers, redwoods, and hardwoods (Jones and Post, 2004). Similarly, a review of 145 deforestation and afforestation studies investigated the estimated changes in annual water yield for seven different kinds of vegetation types—the greatest changes occurred in conifer forests while the smallest changes in annual water yields occurred in scrub dominated catchments (Sahin and Hall, 1996).

Comparatively, peak flow changes were likely due to fire effects on soil hydraulic properties, particularly infiltration. Besides fire severity and proportion of catchment burned, aridity was also identified as an important driver of wildfire-caused peak flow changes (Fig. 8). Partial dependence plots indicated that more arid areas led to higher peak flow changes with wildfire, which was opposite to the relationship between aridity and annual water yield changes (Figs. 9 and 10). Greater peak flows in higher aridity catchments was likely due to aridity acting as a high order control on the curve number in the model, which controls the proportion of runoff. This was particularly interesting because it was consistent with several recent empirical studies. For example, in a study of two burned basins with differing aridities in Victoria, AUS, the more arid basin had infiltration rates 333-times lower and runoff ratios 7-times greater than a wetter basin (Noske et al., 2016). Similarly, in

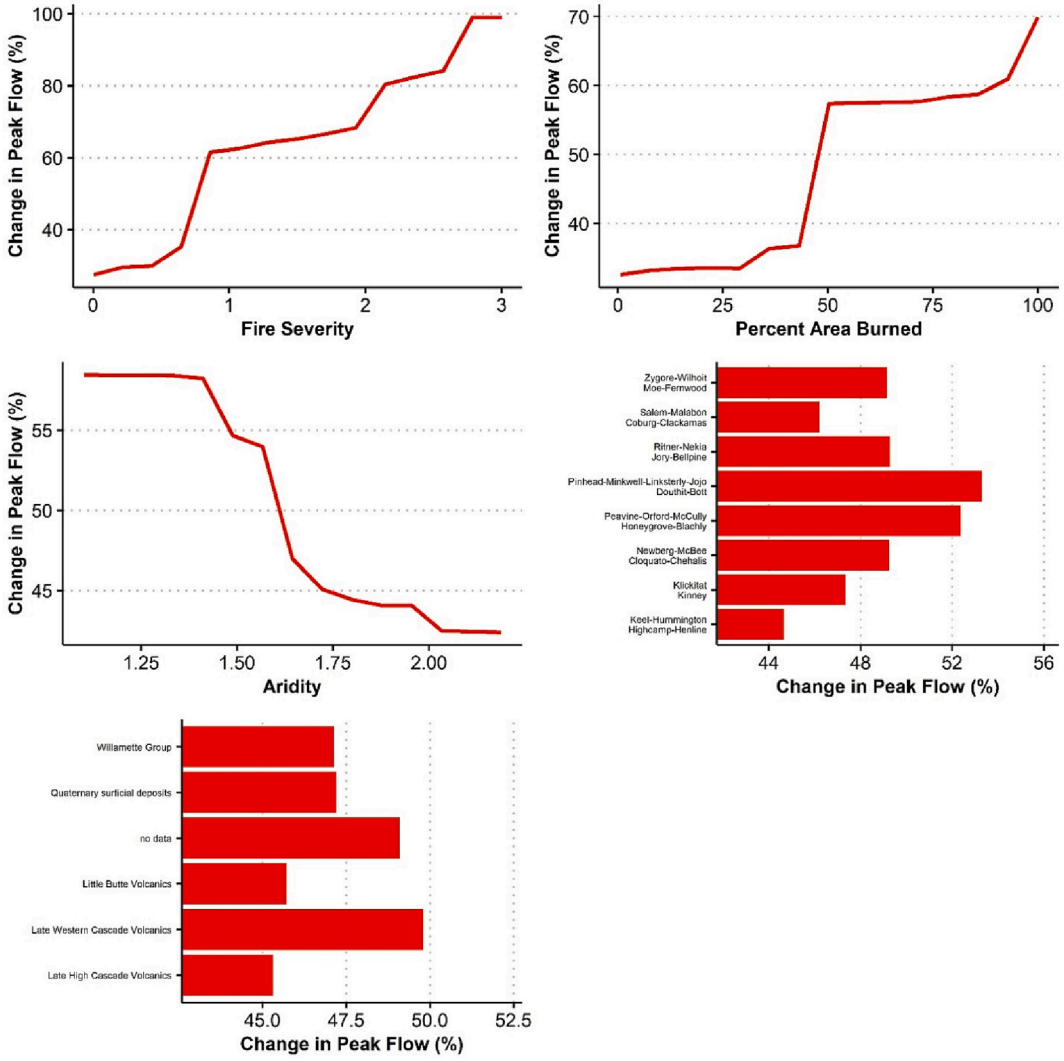

Fig. 10. Partial dependence plots for the five most important variables from the peak streamflow random forest model for the North Santiam and McKenzie basins, Oregon. Plots show the relationship between the variable and relative peak flow change between the burned and unburned scenarios.

five burned plots from Victoria, AUS there was a power relationship between aridity and surface runoff ratio, with runoff ratios two orders of magnitude greater in the driest site compared to the wettest site (Van der Sant et al., 2018).

Besides aridity, infiltration is often also strongly related to soil type, which was determined to be the fourth most important factor describing peak flow changes in our study (Fig. 8). Partial dependence plots predicted the largest peak flow changes in catchments with soil types with low rock fragments and carbon contents (Fig. 10, A2–A3). The inverse relationship between rock content and peak flows was expected as increased preferential flow—where water is transported to depth in soils—is known to occur in coarser soils resulting in lower runoff responses (Hartmann et al., 2020). Several empirical studies have also illustrated the importance of soil properties for post-fire infiltration and runoff changes. For example, an examination of the wettability of different sized soil aggregates from alkaline, calcareous loamy soils in Spain showed that the larger aggregates (1–2 mm) had low levels of hydrophobicity and retained macropores after burning, resulting in less runoff (Mataix-Solera and Doerr, 2004). Additionally, an erosion lag was observed for soils with high gravel contents in a study of seven burned sites in New Mexico, which was attributed to an armoring effect of gravel, increasing infiltration and preventing surface runoff (Ebel et al., 2018); however, unfortunately, armoring is not a process explicitly represented in the model. Additionally, gravel does not always lead to decreased runoff—during the first storm after a wildfire in California, ash filled macropores in gravelly soils, leading to increased runoff ratios (Onda et al., 2008). Our wildfire simulations did not include ash dynamics, which is likely why we did not observe such an effect.

The inverse relationship between carbon content and peak flow was counter to our expectations. Generally, catchments with greater soil carbon retain and store more water (Hudson, 1994). However, our model did not change the soil carbon in the wildfire scenarios, so sites with high soil carbon likely continued to retain the soil water, limiting surface runoff and peak flows. This is counter to what several empirical studies have found. For example, in Northern Mongolia, soil volumetric water content was reduced in soils after wildfire, Kopp et al. (2017) hypothesized that this was due to loss of the organic layer, increasing water movement through preferential flow paths and increasing stormflow. Similarly, water retention was greatly decreased for soils on Southern slopes with higher organic matter contents following a wildfire in Colorado (Ebel, 2012).

Lastly, geologic province was also identified as an important factor for peak flow changes (Fig. 8). This result was not too surprising. For unburned conditions at our sites, surface runoff is extremely limited and most peak flows are generated by subsurface stormflow. While we did observe an increase in runoff with wildfire, we would still expect those subsurface processes to remain important. Partial dependence plots identified the smallest post-fire peak flow changes for High Cascades geology while Western Cascades geology showed the greatest changes (Fig. 10). High Cascades province has highly permeable rocks, lacks drainage networks, and is primarily spring fed, with groundwater transit times between 3 and 26 years (Jefferson et al., 2007, 2006). Comparatively, Western Cascades is dominated by low permeability rocks, steep slopes, and streamflow is primarily from shallow subsurface flows (Jefferson et al., 2007, 2006). These differences are likely leading to differing peak flow responses after wildfire. This was also observed in a Northern California modeling study which tested how wildfire location impacted runoff and infiltration; the greatest changes occurred in areas with sleep, complex topography in areas with low permeability (Maina and Siirila-Woodburn, 2020). Additionally, the long flow path timescales in the High Cascades likely helps to delay or mute the effect of wildfire entirely. This was noted for two burned catchments in Southern California where end member mixing analysis was used to investigate the subsurface response to wildfire (Jung et al., 2009). The basin with greater groundwater contributions prior to the fire showed a more muted response to wildfire, with surface runoff only increasing by a mean of 2.8 %, comparatively, surface runoff increased by a mean of 41.4 % in the basin where flow is split evenly between soil water and groundwater.

Wildfire effects on streamflow were substantially greater at the headwater scale than the basin outlet. Our models predicted annual water yield changes between −0.25–155 % for headwater subbasins and 1.28–23.4 % at the basin scale (Fig. 7). For basins less than 10,000 ha—the approximate area of our modeled headwater subbasins—measured changes in annual streamflow have ranged from 20 to 450 % in empirical studies (Campbell et al., 1977; Hallema et al., 2017a; Helvey, 1980; Lane et al., 2006; Loáiciga et al., 2001; Owens et al., 2013; Scott, 1997; Wine and Cadol, 2016) and 1.2–74.6 % in modeling studies (Havel et al., 2018). Similar to our model results, wildfire effects observed in empirical studies have tended to be smaller at larger basin scales (>10,000 ha), ranging from no change up to a 38 % increase in annual water yields in basins up to 122,300 ha in area (Bart, 2016; Bart and Hope, 2010; Hallema et al., 2017a; Lane et al., 2006; Loáiciga et al., 2001; Owens et al., 2013; Scott, 1997; Wine and Cadol, 2016). In other modeling studies, post-fire annual water yields have been estimated to increase 0.7–63.7 %, although most models have projected annual water yield increases of less than 10 % (Basso et al., 2020; Havel et al., 2018; Loiselle et al., 2020; Morán-Tejeda et al., 2015).

Comparatively, peak flows in our models were predicted to change between −0.78–520 % at the headwater subbasin scale and −1.1–50.9 % at the larger basin scale (Fig. 7). Previous modeling studies have also projected a substantial range in potential peak flows responses, ranging between 120 and 2,725 % for basins less than 2,500 ha (Seibert et al., 2010; Sidman et al., 2015). These model projections seem to align with empirical studies, which have also observed substantial variability in post-fire peak flows. For example, in small basins (less than 10 ha), increases in post-fire peak flows ranged between 0 and 14,200 % (Campbell et al., 1977). In moderate to larger basins (>300 ha) observations of peak flow increases have ranged from 5 to 850 % (Mahat et al., 2016; Niemeyer et al., 2020; Scott, 1997; Soulis et al., 2012). Indeed, much of the variability in both model and empirical results during the immediate post-fire years is likely related to the temporal alignment of precipitation intensity, precipitation duration, soil water content, and soil hydraulic properties (Moody and Martin, 2001; Thomas et al., 2021). However, in our analysis of post-fire flow drivers, we focused primarily on long-term climate and landscape conditions, so effects of these short-scale processes were not considered. Additionally, in catchments with reservoirs, peak flow responses may be mediated by water managers decreasing reservoir outflows to reduce the potential for downstream flooding.

Across the range of precipitation scenarios our model was not always able to capture post-fire observed peak flows, particularly in the timing of the peaks (Fig. 4). This was likely because the SWAT model was not originally designed for predicting wildfire effects and was not able to capture all of the physical landscape changes that occur with wildfire. While our fire module was developed to improve existing methods of representing fire in the SWAT model, more work is needed to refine the representation of wildfire effects on the physical processes within the model. For instance, in building the fire simulation we changed the land use to account for the decrease in ET often observed post-fire. In catchments burned at high severity, it is reasonable to assume ET rates will decrease due to the loss of vegetation (Ma et al., 2020). However, in catchments burned at low to moderate burn severity, ET may remain unchanged (Poulos et al., 2021) or even increase post-fire due to compensatory transpiration from the remaining vegetation (Nolan et al., 2014). Another way to represent post-fire ET changes would have been to adjust the leaf area index and rooting depth within the model, however these parameters were found to be insensitive in our models. Lastly, future studies might consider using more complex runoff representations like the Green-Ampt equation to more accurately represent infiltration excess runoff or SWAT-VSA to more accurately represent the effects of topographic convergence on runoff processes (Easton et al.,

2008). Future refinements of hydrologic models to more accurately represent the effects of wildfire on vegetation and soil characteristics may provide more accurate post-fire streamflow predictions.

Additionally, we noted poor NSE values for many of the smaller headwater catchments (Table S1). Fortunately, these were principally located in unburned catchments, upstream of our area of focus and were not included in our analysis. The poor model simulations in these catchments were likely due to the unique and complex hydrologic flow paths in the catchments in this region—streamflow is often discontinuous with substantial groundwater contributions, which are poorly represented in all hydrologic models.

5. Conclusions

In our study, we modeled two recently burned basins in Oregon to project the range of effects on streamflow both at the headwater and downstream scale. Post-fire increases in annual water yields, peaks flows, and low flows were projected to be greatest in headwater catchments, but more muted at the downstream basin scale. The post-fire hydrological response was most strongly related to burn severity, catchment area burned, and annual precipitation. However, catchment aridity, vegetation type, soil type, and geology were also important drivers. The influence of a broad range of burn characteristics, catchment characteristics, and climatic factors highlights the substantial uncertainty that remains regarding the initial hydrologic responses to wildfire.

As the occurrence of large, high severity wildfires has increased in many regions across the planet, it is increasingly critical to improve hydrologic model projections. Post-fire shifts in water quantity and quality can create substantial and costly challenges for downstream drinking water treatment and aquatic ecosystem health. Unfortunately, the majority of hydrologic models were not originally developed to include the unique impacts of wildfire. As such, we require additional efforts to continue to improve model projections of post-fire changes in hydrologic processes. Future research should leverage unfortunate, but rare, opportunities to quantify post-fire hydrologic responses to provide improvements to model parameterization and calibration. Empirical data may also be used to test results in real world conditions, since modeling is a simplified representation of the real world and cannot encompass all of the complexities of a landscape.

CRediT authorship contribution statement

K.A. Wampler: Conceptualization, Methodology, Formal analysis, Investigation, Writing – original draft, Writing – review & editing, Visualization. **K.D. Bladon:** Conceptualization, Resources, Writing – original draft, Writing – review & editing, Supervision, Project administration, Funding acquisition. **M. Faramarzi:** Software, Writing – review & editing.

Declaration of Competing Interest

The authors declare that they have no known competing financial interests or personal relationships that could have appeared to influence the work reported in this paper.

Data availability

The authors do not have permission to share data.

Acknowledgments

Thank you to Majid Zaremehrjardy for all your help writing the code for the fire module. Thanks to Brian Ebel, David Donahue, Karl Morgenstern, Susan Fricke, and Lisa Erkert for valuable discussions and feedback on the research design and assistance with data wrangling. This material is partially based upon work supported by the H.J. Andrews Experimental Forest and Long Term Ecological Research (LTER) program under the NSF grant LTER8 DEB-2025755.

The authors declare no conflicts of interest relevant to this study.

Funding

Wampler was supported by the Rick Strachan Forest Engineering Graduate Fellowship and AWWA Larson Aquatic Research Support Scholarship. Bladon and Wampler were also partially supported by the Department of Energy, Pacific Northwest National Laboratory [Award #608983] and the USDA Forest Service [Agreement #22-JV-11261952-071]. Faramarzi was supported by the Campus Alberta Innovation Program Chair grant to MF [Grant #RES0034497].

Appendix A. Supplementary data

Supplementary data to this article can be found online at https://doi.org/10.1016/j.jhydrol.2023.129585.

References

Abatzoglou, J.T., Brown, T.J., 2012. A comparison of statistical downscaling methods suited for wildfire applications. Int. J. Climatol. 32, 772–780. https://doi.org/10.1002/joc.2312.

Abatzoglou, J.T., Juang, C.S., Williams, A.P., Kolden, C.A., Westerling, A.L., 2021. Increasing Synchronous Fire Danger in Forests of the Western United States. Geophys. Res. Lett. 48, e2020GL091377. doi: 10.1029/2020GL091377.

Abatzoglou, J.T., Williams, A.P., Boschetti, L., Zubkova, M., Kolden, C.A., 2018. Global patterns of interannual climate–fire relationships. Glob. Change Biol. 24, 5164–5175. https://doi.org/10.1111/gcb.14405.

Alauzis, M.V., Mazzarino, M.J., Raffaele, E., Roselli, L., 2004. Wildfires in NW Patagonia: long-term effects on a Nothofagus forest soil. For. Ecol. Manag. 192, 131–142. https://doi.org/10.1016/j.foreco.2003.11.014.

Badía, D., Martí, C., 2003. Plant ash and heat intensity effects on chemical and physical properties of two contrasting soils. Arid Land Res. Manag. 17, 23–41. https://doi.org/10.1080/15324980301595.

Balfour, V.N., Doerr, S.H., Robichaud, P.R., 2014. The temporal evolution of wildfire ash and implications for post-fire infiltration. Int. J. Wildland Fire 23, 733–745. https://doi.org/10.1071/WF13159.

Bart, R.R., 2016. A regional estimate of postfire streamflow change in California. Water Resour. Res. 52, 1465–1478. https://doi.org/10.1002/2014WR016553.

Bart, R.R., Hope, A., 2010. Streamflow response to fire in large catchments of a Mediterranean-climate region using paired-catchment experiments. J. Hydrol. 388, 370–378. https://doi.org/10.1016/j.jhydrol.2010.05.016.

Basso, M., Vieira, D.C.S., Ramos, T.B., Mateus, M., 2020. Assessing the adequacy of SWAT model to simulate postfire effects on the watershed hydrological regime and water quality. Land Degrad. Dev. 31, 619–631. https://doi.org/10.1002/ldr.3476.

BC Wildfire Service, n.d. Wildfire Averages [WWW Document]. URL https://www2.gov.bc.ca/gov/content/safety/wildfire-status/about-bcws/wildfire-statistics/wildfire-averages (accessed 11.16.20).

Bladon, K.D., 2018. Rethinking wildfires and forest watersheds. Science 359, 1001–1002. https://doi.org/10.1126/science.aar8120.

Bladon, K.D., Silins, U., Wagner, M.J., Stone, M., Emelko, M.B., Mendoza, C.A., Devito, K. J., Boon, S., 2008. Wildfire impacts on nitrogen concentration and production from headwater streams in southern Alberta's Rocky Mountains. Can. J. For. Res. 38, 2359–2371. https://doi.org/10.1139/X08-071.

Bladon, K.D., Emelko, M.B., Silins, U., Stone, M., 2014. Wildfire and the future of water supply. Environ. Sci. Technol. 48, 8936–8943. https://doi.org/10.1021/es500130g.

Bladon, K.D., Bywater-Reyes, S., LeBoldus, J.M., Keriö, S., Segura, C., Ritóková, G., Shaw, D.C., 2019. Increased streamflow in catchments affected by a forest disease epidemic. Sci. Total Environ. 691, 112–123. https://doi.org/10.1016/j.scitotenv.2019.07.127.

Bodí, M.B., Doerr, S.H., Cerdà, A., Mataix-Solera, J., 2012. Hydrological effects of a layer of vegetation ash on underlying wettable and water repellent soil. Geoderma, Fire effects on soil properties 191, 14–23. https://doi.org/10.1016/j.geoderma.2012.01.006.

Boer, M., Dios, V., Bradstock, R., 2020. Unprecedented burn area of Australian mega forest fires. Nat. Clim. Change 10, 1–2. https://doi.org/10.1038/s41558-020-0716-1.

Boisrame, G.F.S., Thompson, S.E., Tague, C., Stephens, S.L., 2019. Restoring a natural fire regime alters the water balance of a Sierra Nevada catchment. Water Resour. Res. 55, 5751–5769. https://doi.org/10.1029/2018wr024098.

Borah, D.K., Bera, M., 2004. Watershed-scale hydrologic and nonpoint-source pollution models: review of applications. Trans. ASAE 47, 789–803.

Bradford, M.J., Heinonen, J.S., 2008. Low flows, instream flow needs and fish ecology in small streams. Can. Water Resour. J. 33, 165–180. https://doi.org/10.4296/cwrj3302165.

Brooks, J.R., Meinzer, F.C., Warren, J.M., Domec, J.-C., Coulombe, R., 2006. Hydraulic redistribution in a Douglas-fir forest: lessons from system manipulations. Plant Cell Environ. 29, 138–150. https://doi.org/10.1111/j.1365-3040.2005.01409.x.
Campbell, R.E., Baker, J., Ffolliott, P.F., Larson, F.R., Avery, C.C., 1977. Wildfire effects on a ponderosa pine ecosystem: An Arizona case study (No. RM-191), Research Paper (RP). USDA Forest Service, Fort Collins, CO.
Certini, G., 2005. Effects of fire on properties of forest soils: a review. Oecologia 143, 1–10.
Committee on Hydrologic Impacts of Forest Management, 2008. Hydrologic Effects of a Changing Forest Landscape. The National Academies Press, Washington, D.C.
Congressional Research Service, 2021. Wildfire Statistics (No. IF10244). Washington, DC.
Coombs, J.S., Melack, J.M., 2013. Initial impacts of a wildfire on hydrology and suspended sediment and nutrient export in California chaparral watersheds. Hydrol. Process. 27, 3842–3851. https://doi.org/10.1002/hyp.9508.
Costanza, R., d'Arge, R., de Groot, R., Farber, S., Grasso, M., Hannon, B., Limburg, K., Naeem, S., O'Neill, R.V., Paruelo, J., Raskin, R.G., Sutton, P., van den Belt, M., 1997. The value of the world's ecosystem services and natural capital. Nature 387, 253–260. https://doi.org/10.1038/387253a0.
Daly, C., Schulze, M.D., McKee, W.A., 2020. Meteorological data from benchmark stations at the HJ Andrews Experimental Forest, 1957 to present. Long-Term Ecological Research. Forest Science Data Bank, Corvallis, OR. [Database].
Delpla, I., Jung, A.-V., Baures, E., Clement, M., Thomas, O., 2009. Impacts of climate change on surface water quality in relation to drinking water production. Environ. Int. 35, 1225–1233. https://doi.org/10.1016/j.envint.2009.07.001.
Dobre, M., Srivastava, A., Lew, R., Deval, C., Brooks, E.S., Elliot, W.J., Robichaud, P.R., 2022. WEPPcloud: An online watershed-scale hydrologic modeling tool. Part II. Model performance assessment and applications to forest management and wildfires. J. Hydrol. 610, 18. https://doi.org/10.1016/j.jhydrol.2022.127776.
Domec, J.-C., Warren, J.M., Meinzer, F.C., Brooks, J.R., Coulombe, R., 2004. Native root xylem embolism and stomatal closure in stands of Douglas-fir and ponderosa pine: mitigation by hydraulic redistribution. Oecologia 141, 7–16. https://doi.org/10.1007/s00442-004-1621-4.
Domec, J.-C., Lachenbruch, B., Meinzer, F.C., Woodruff, D.R., Warren, J.M., McCulloh, K. A., 2008. Maximum height in a conifer is associated with conflicting requirements for xylem design. Proc. Natl. Acad. Sci. https://doi.org/10.1073/pnas.0710418105.
Du, X., Loiselle, D., Alessi, D.S., Faramarzi, M., 2020. Hydro-climate and biogeochemical processes control watershed organic carbon inflows: Development of an in-stream organic carbon module coupled with a process-based hydrologic model. Sci. Total Environ. 718, 137281 https://doi.org/10.1016/j.scitotenv.2020.137281.
Dudley, N., Stolton, S., 2003. Running pure: the importance of forest protected areas to drinking water.
Ebel, B.A., 2012. Wildfire impacts on soil-water retention in the Colorado Front Range, United States. Water Resour. Res. 48 https://doi.org/10.1029/2012WR012362.
Ebel, B.A., 2013. Wildfire and aspect effects on hydrologic states after the 2010 Fourmile Canyon fire. Vadose Zone J. 12, 1–19. https://doi.org/10.2136/vzj2012.0089.
Ebel, B.A., Mirus, B.B., 2014. Disturbance hydrology: challenges and opportunities. Hydrol. Process. 28, 5140–5148. https://doi.org/10.1002/hyp.10256.
Ebel, B.A., Moody, J.A., Martin, D.A., 2012. Hydrologic conditions controlling runoff generation immediately after wildfire. Water Resour. Res. 48 https://doi.org/10.1029/2011WR011470.
Ebel, B.A., Moody, J.A., 2017. Synthesis of soil-hydraulic properties and infiltration timescales in wildfire-affected soils. Hydrol. Process. 31, 324–340. https://doi.org/10.1002/hyp.10998.
Ebel, B.A., Moody, J.A., 2020. Parameter estimation for multiple post-wildfire hydrologic models. Hydrol. Process. 34, 4049–4066. https://doi.org/10.1002/hyp.13865.
Ebel, B.A., Romero, O.C., Martin, D.A., 2018. Thresholds and relations for soil-hydraulic and soil-physical properties as a function of burn severity 4 years after the 2011 Las Conchas Fire, New Mexico, USA. Hydrol. Process. 32, 2263–2278. https://doi.org/10.1002/hyp.13167.
Ebel, B.A., Shephard, Z.M., Walvoord, M.A., Murphy, S.F., Partridge, T.F., Perkins, K.S., 2023. Modeling post-wildfire hydrologic response: review and future directions for applications of physically based distributed simulation. Earth Future 11 (2), 23. https://doi.org/10.1029/2022ef003038.
Emelko, M.B., Silins, U., Bladon, K.D., Stone, M., 2011. Implications of land disturbance on drinking water treatability in a changing climate: demonstrating the need for "source water supply and protection" strategies. Water Res. 45, 461–472. https://doi.org/10.1016/j.watres.2010.08.051.
Emelko, M.B., Stone, M., Silins, U., Allin, D., Collins, A.L., Williams, C.H.S., Martens, A. M., Bladon, K.D., 2016. Sediment-phosphorus dynamics can shift aquatic ecology and cause downstream legacy effects after wildfire in large river systems. Glob. Change Biol. 22, 1168–1184. https://doi.org/10.1111/gcb.13073.
Emmerton, C.A., Cooke, C.A., Hustins, S., Silins, U., Emelko, M.B., Lewis, T., Kruk, M.K., Taube, N., Zhu, D., Jackson, B., Stone, M., Kerr, J.G., Orwin, J.F., 2020. Severe western Canadian wildfire affects water quality even at large basin scales. Water Res. 183, 116071 https://doi.org/10.1016/j.watres.2020.116071.
Fan, Y., Miguez-Macho, G., Jobbágy, E.G., Jackson, R.B., Otero-Casal, C., 2017. Hydrologic regulation of plant rooting depth. Proc. Natl. Acad. Sci. 114, 10572–10577. https://doi.org/10.1073/pnas.1712381114.
Faramarzi, M., Srinivasan, R., Iravani, M., Bladon, K.D., Abbaspour, K.C., Zehnder, A.J. B., Goss, G.G., 2015. Setting up a hydrological model of Alberta: Data discrimination analyses prior to calibration. Environ. Model. Softw. 74, 48–65. https://doi.org/10.1016/j.envsoft.2015.09.006.
Feikema, P.M., Sherwin, C.B., Lane, P.N.J., 2013. Influence of climate, fire severity and forest mortality on predictions of long term streamflow: Potential effect of the 2009 wildfire on Melbourne's water supply catchments. J. Hydrol. 488, 1–16. https://doi.org/10.1016/j.jhydrol.2013.02.001.
Filkov, A., Ngo, T., Matthews, S., Telfer, S., Penman, T., 2020. Impact of Australia's catastrophic 2019/20 bushfire season on communities and environment. Retrospective analysis and current trends. J. Saf. Sci. Resil. 1, 44–56. https://doi.org/10.1016/j.jnlssr.2020.06.009.
Flannigan, M.D., Krawchuk, M.A., de Groot, W.J., Wotton, B.M., Gowman, L.M., 2009. Implications of changing climate for global wildland fire. Int. J. Wildland Fire 18, 483–507. https://doi.org/10.1071/WF08187.
Flannigan, M.D., Cantin, A.S., de Groot, W.J., Wotton, M., Newbery, A., Gowman, L.M., 2013. Global wildland fire season severity in the 21st century. For. Ecol. Manag., The Mega-fire reality 294, 54–61. https://doi.org/10.1016/j.foreco.2012.10.022.
García-Corona, R., Benito, E., de Blas, E., Varela, M.E., 2004. Effects of heating on some soil physical properties related to its hydrological behaviour in two north-western Spanish soils. Int. J. Wildland Fire 13, 195–199. https://doi.org/10.1071/WF03068.
Gassman, P., Reyes, M., Green, C., Arnold, J., 2007. The soil and water assessment tool: historical development, applications, and future research directions. Trans. ASABE 50, 1211–1250. https://doi.org/10.13031/2013.23637.
Geographic Area Coordination Center, 2020. National Large Incident Year-to-Date Report.
Grayson, R.B., Moore, I.D., McMahon, T.A., 1992. Physically based hydrologic modeling: Is the concept realistic? Water Resour. Water Resour. Res. 28, 2659–2666. https://doi.org/10.1029/92WR01259.
Greenwell, B.M., 2017. pdp: an R package for constructing partial dependence plots. R J. 9, 421–436.
Hallema, D.W., Sun, G., Bladon, K.D., Norman, S.P., Caldwell, P.V., Liu, Y., McNulty, S. G., 2017a. Regional patterns of postwildfire streamflow response in the Western United States: the importance of scale-specific connectivity. Hydrol. Process. 31, 2582–2598. https://doi.org/10.1002/hyp.11208.
Hallema, D.W., Sun, G., Caldwell, P.V., Norman, S.P., Cohen, E.C., Liu, Y., Ward, E.J., McNulty, S.G., 2017b. Assessment of wildland fire impacts on watershed annual water yield: analytical framework and case studies in the United States. Ecohydrology 10, e1794.
Hallema, D.W., Robinne, F.-N., Bladon, K.D., 2018. Reframing the Challenge of Global Wildfire Threats to Water Supplies. Earths Future 6, 772–776. https://doi.org/10.1029/2018EF000867.
Halofsky, J.E., Peterson, D.L., Harvey, B.J., 2020. Changing wildfire, changing forests: the effects of climate change on fire regimes and vegetation in the Pacific Northwest, USA. Fire Ecol. 16, 4. https://doi.org/10.1186/s42408-019-0062-8.
Hartmann, A., Semenova, E., Weiler, M., Blume, T., 2020. Field observations of soil hydrological flow path evolution over 10 millennia. Hydrol. Earth Syst. Sci. 24, 3271–3288. https://doi.org/10.5194/hess-24-3271-2020.
Havel, A., Tasdighi, A., Arabi, M., 2018. Assessing the hydrologic response to wildfires in mountainous regions. Hydrol. Earth Syst. Sci. 22, 2527–2550. https://doi.org/10.5194/hess-22-2527-2018.
Helsel, D.R., Hirsch, R.M., Ryberg, K.R., Archfield, S.A., Gilroy, E.J., 2020. Statistical methods in water resources (USGS Numbered Series No. 4-A3), Statistical methods in water resources, Techniques and Methods. U.S. Geological Survey, Reston, VA. doi: 10.3133/tm4A3.
Helvey, J.D., 1980. Effects of a North Central Washington Wildfire on Runoff and Sediment Production1. J. Am. Water Resour. Assoc. 16, 627–634. https://doi.org/10.1111/j.1752-1688.1980.tb02441.x.
Henley, J., Jones, S., 2019. Spain Battles Biggest Wildfires in 20 Years as Heatwave Grips Europe. The Gaurdian.
Hohner, A.K., Rhoades, C.C., Wilkerson, P., Rosario-Ortiz, F.L., 2019. Wildfires alter forest watersheds and threaten drinking water quality. Acc. Chem. Res. 52, 1234–1244. https://doi.org/10.1021/acs.accounts.8b00670.
Hothorn, T., Bühlmann, P., Dudoit, S., Molinaro, A., Van Der Laan, M.J., 2006. Survival ensembles. Biostatistics 7, 355–373. https://doi.org/10.1093/biostatistics/kxj011.
Hudson, B.D., 1994. Soil organic matter and available water capacity. J. Soil Water Conserv. 49, 189.
Jefferson, A., Grant, G., Lewis, S., 2007. A river runs underneath it: geologic control of spring and channel systems and management implications, Cascade Range, Oregon. pp. 391–400.
Jefferson, A., Grant, G., Rose, T., 2006. Influence of volcanic history on groundwater patterns on the west slope of the Oregon High Cascades. Water Resour. Res. 42 https://doi.org/10.1029/2005WR004812.
Jefferson, A., 2006. Hydrology and Geomorphic Evolution of Basaltic Landscapes, High Cascades, Oregon. Oregon State University, Corvallis, OR.
Jones, J.A., Post, D.A., 2004. Seasonal and successional streamflow response to forest cutting and regrowth in the northwest and eastern United States. Water Resour. Res. 40 https://doi.org/10.1029/2003WR002952.
Jung, H.Y., Hogue, T.S., Rademacher, L.K., Meixner, T., 2009. Impact of wildfire on source water contributions in Devil Creek, CA: evidence from end-member mixing analysis. Hydrol. Process. 23, 183–200. https://doi.org/10.1002/hyp.7132.
Keeley, J.E., 2009. Fire intensity, fire severity and burn severity: a brief review and suggested usage. Int. J. Wildland Fire 18, 116–126. https://doi.org/10.1071/WF07049.
Khan, S.J., Deere, D., Leusch, F.D.L., Humpage, A., Jenkins, M., Cunliffe, D., 2015. Extreme weather events: Should drinking water quality management systems adapt to changing risk profiles? Water Res. 85, 124–136. https://doi.org/10.1016/j.watres.2015.08.018.
Kinoshita, A.M., Hogue, T.S., Napper, C., 2014. Evaluating pre- and post-fire peak discharge predictions across Western U.S. Watersheds. JAWRA J. Am. Water Resour. Assoc. 50, 1540–1557. https://doi.org/10.1111/jawr.12226.

Kinoshita, A.M., Hogue, T.S., 2015. Increased dry season water yield in burned watersheds in Southern California. Environ. Res. Lett. 10, 014003 https://doi.org/10.1088/1748-9326/10/1/014003.
Kottek, M., Grieser, J., Beck, C., Rudolf, B., Rubel, F., 2006. World Map of the Köppen-Geiger climate classification updated. Meteorol. Z. 15, 259–263. https://doi.org/10.1127/0941-2948/2006/0130.
Kurz, W.A., Dymond, C.C., Stinson, G., Rampley, G.J., Neilson, E.T., Carroll, A.L., Ebata, T., Safranyik, L., 2008. Mountain pine beetle and forest carbon feedback to climate change. Nature 452, 987–990. https://doi.org/10.1038/nature06777.
Kusaka, S., Nakane, K., Mitsudera, M., 1983. Effect of fire on water and major nutrient budgets in forest ecosystems: I. Water balance. Jpn. J. Ecol. 33, 323–332. https://doi.org/10.18960/seitai.33.3_323.
Lane, P.N.J., Sheridan, G.J., Noske, P.J., 2006. Changes in sediment loads and discharge from small mountain catchments following wildfire in south eastern Australia. J. Hydrol. 331, 495–510. https://doi.org/10.1016/j.jhydrol.2006.05.035.
Larsen, I.J., MacDonald, L.H., Brown, E., Rough, D., Welsh, M.J., Pietraszek, J.H., Libohova, Z., Benavides-Solorio, J. de D., Schaffrath, K., 2009. Causes of post-fire runoff and erosion: water repellency, cover, or soil sealing? Soil Sci. Soc. Am. J. 73, 1393–1407. doi: 10.2136/sssaj2007.0432.
Lavee, H., Kutiel, P., Segev, M., Benyamini, Y., 1995. Effect of surface roughness on runoff and erosion in a mediterranean ecosystem: the role of fire. Geomorphology 11, 227–234. https://doi.org/10.1016/0169-555X(94)00059-Z.
Lenth, R.V., 2021. emmeans: Estimated Marginal Means, aka Least-Squares Means.
Li, Q., Wei, X., Zhang, M., Liu, W., Fan, H., Zhou, G., Giles-Hansen, K., Liu, S., Wang, Y., 2017. Forest cover change and water yield in large forested watersheds: A global synthetic assessment. Ecohydrology 10, e1838.
Loáiciga, H.A., Pedreros, D., Roberts, D., 2001. Wildfire-streamflow interactions in a chaparral watershed. Adv. Environ. Res. 5, 295–305. https://doi.org/10.1016/S1093-0191(00)00064-2.
Loiselle, D., Du, X., Alessi, D.S., Bladon, K.D., Faramarzi, M., 2020. Projecting impacts of wildfire and climate change on streamflow, sediment, and organic carbon yields in a forested watershed. J. Hydrol. 590, 125403 https://doi.org/10.1016/j.jhydrol.2020.125403.
Lund, J.R., Palmer, R.N., 1997. Water resource system modeling for conflict resolution. Water Resour. Update 3, 70–82.
Lutes, D.C., Keane, R.E., Caratti, J.F., Key, C.H., Benson, N.C., Sutherland, S., Gangi, L.J., 2006. FIREMON: Fire effects monitoring and inventory system (No. RMRS-GTR-164). U.S. Department of Agriculture, Forest Service, Rocky Mountain Research Station, Ft. Collins, CO. doi: 10.2737/RMRS-GTR-164.
Ma, Q., Bales, R.C., Rungee, J., Conklin, M.H., Collins, B.M., Goulden, M.L., 2020. Wildfire controls on evapotranspiration in California's Sierra Nevada. J. Hydrol. 590, 125364 https://doi.org/10.1016/j.jhydrol.2020.125364.
Mahat, V., Silins, U., Anderson, A., 2016. Effects of wildfire on the catchment hydrology in southwest Alberta. CATENA 147, 51–60. https://doi.org/10.1016/j.catena.2016.06.040.
Maina, F.Z., Siirila-Woodburn, E.R., 2020. Watersheds dynamics following wildfires: Nonlinear feedbacks and implications on hydrologic responses. Hydrol. Process. 34, 33–50. https://doi.org/10.1002/hyp.13568.
Malvar, M.C., Prats, S.A., Nunes, J.P., Keizer, J.J., 2011. Post-fire overland flow generation and inter-rill erosion under simulated rainfall in two eucalypt stands in north-central Portugal. Environ. Res., Fire Effects on Soil Properties: Forest Fires and Prescribed Fires 111, 222–236. https://doi.org/10.1016/j.envres.2010.09.003.
Marlon, J.R., Bartlein, P.J., Gavin, D.G., Long, C.J., Anderson, R.S., Briles, C.E., Brown, K.J., Colombaroli, D., Hallett, D.J., Power, M.J., Scharf, E.A., Walsh, M.K., 2012. Long-term perspective on wildfires in the western USA. Proc. Natl. Acad. Sci. 109, E535–E543. doi: 10.1073/pnas.1112839109.
Martin, D.A., 2016. At the nexus of fire, water and society. Philos. Trans. R. Soc. B Biol. Sci. 371, 20150172. https://doi.org/10.1098/rstb.2015.0172.
Mast, M.A., Murphy, S.F., Clow, D.W., Penn, C.A., Sexstone, G.A., 2016. Water-quality response to a high-elevation wildfire in the Colorado Front Range. Hydrol. Process. 30, 1811–1823. https://doi.org/10.1002/hyp.10755.
Mataix-Solera, J., Doerr, S.H., 2004. Hydrophobicity and aggregate stability in calcareous topsoils from fire-affected pine forests in southeastern Spain. Geoderma 118, 77–88. https://doi.org/10.1016/S0016-7061(03)00185-X.
Mayer, T.D., 2012. Controls of summer stream temperature in the Pacific Northwest. J. Hydrol. 475, 323–335. https://doi.org/10.1016/j.jhydrol.2012.10.012.
McGuire, L.A., Rengers, F.K., Kean, J.W., Staley, D.M., 2017. Debris flow initiation by runoff in a recently burned basin: Is grain-by-grain sediment bulking or en masse failure to blame? Geophys. Res. Lett. 44 (14), 7310–7319. https://doi.org/10.1002/2017gl074243.
Meng, R., Dennison, P.E., Huang, C., Moritz, M.A., D'Antonio, C., 2015. Effects of fire severity and post-fire climate on short-term vegetation recovery of mixed-conifer and red fir forests in the Sierra Nevada Mountains of California. Remote Sens. Environ. 171, 311–325. https://doi.org/10.1016/j.rse.2015.10.024.
Mikkelson, K.M., Dickenson, E.R.V., Maxwell, R.M., McCray, J.E., Sharp, J.O., 2013. Water-quality impacts from climate-induced forest die-off. Nat. Clim. Change 3, 218–222. https://doi.org/10.1038/nclimate1724.
Mirchi, A., Watkins, D., Madani, K., 2010. Modeling for watershed planning, management, and decision making. In: Vaughn, J.C. (Ed.), Watersheds: Management, Restoration and Environmental Impact. Nova Science Publishers, Hauppauge, New York, pp. 1–25.
Monitoring Trends in Burn Severity, n.d. Post-Fire Mapping Glossary [WWW Document]. URL https://burnseverity.cr.usgs.gov/glossary (accessed 11.17.22).
Moody, J.A., Ebel, B.A., 2012. Hyper-dry conditions provide new insights into the cause of extreme floods after wildfire. CATENA 93, 58–63. https://doi.org/10.1016/j.catena.2012.01.006.
Moody, J.A., Ebel, B.A., 2014. Infiltration and runoff generation processes in fire-affected soils. Hydrol. Process. 28, 3432–3453. https://doi.org/10.1002/hyp.9857.
Moody, J.A., Martin, D.A., 2001. Initial hydrologic and geomorphic response following a wildfire in the Colorado Front Range. Earth Surf. Process. Landf. 26 (10), 1049–1070. https://doi.org/10.1002/esp.253.
Moody, J.A., Martin, D.A., Haire, S.L., Kinner, D.A., 2008. Linking runoff response to burn severity after a wildfire. Hydrol. Process. 22, 2063–2074. https://doi.org/10.1002/hyp.6806.
Moody, J.A., Shakesby, R.A., Robichaud, P.R., Cannon, S.H., Martin, D.A., 2013. Current research issues related to post-wildfire runoff and erosion processes. Earth-Sci. Rev. 122, 10–37. https://doi.org/10.1016/j.earscirev.2013.03.004.
Moody, J.A., Ebel, B.A., Nyman, P., Martin, D.A., Stoof, C.R., McKinley, R., 2016. Relations between soil hydraulic properties and burn severity. Int. J. Wildland Fire 25, 279293. https://doi.org/10.1071/WF14062.
Morán-Tejeda, E., Zabalza, J., Rahman, K., Gago-Silva, A., López-Moreno, J.I., Vicente-Serrano, S., Lehmann, A., Tague, C.L., Beniston, M., 2015. Hydrological impacts of climate and land-use changes in a mountain watershed: uncertainty estimation based on model comparison. Ecohydrology 8, 1396–1416. https://doi.org/10.1002/eco.1590.
Moriasi, D., Gitau, M., Pai, N., Daggupati, P., 2015. Hydrologic and water quality models: performance measures and evaluation criteria. Trans. ASABE 58, 1763–1785. https://doi.org/10.13031/trans.58.10715.
Moritz, M.A., Parisien, M.-A., Batllori, E., Krawchuk, M.A., Dorn, J.V., Ganz, D.J., Hayhoe, K., 2012. Climate change and disruptions to global fire activity. Ecosphere 3, 1–22. https://doi.org/10.1890/ES11-00345.1.
Murdoch, P.S., Baron, J.S., Miller, T.L., 2000. Potential effects of climate change on surface-water quality in North America1. J. Am. Water Resour. Assoc. 36, 347–366. https://doi.org/10.1111/j.1752-1688.2000.tb04273.x.
Murphy, S.F., Writer, J.H., McCleskey, R.B., Martin, D.A., 2015. The role of precipitation type, intensity, and spatial distribution in source water quality after wildfire. Environ. Res. Lett. 10, 084007 https://doi.org/10.1088/1748-9326/10/8/084007.
Murphy, B.P., Yocom, L.L., Belmont, P., 2018. Beyond the 1984 perspective: narrow focus on modern wildfire trends underestimates future risks to water security. Earths Future 6, 1492–1497. https://doi.org/10.1029/2018EF001006.
National Climatic Data Center, n.d. Climate Data Online [WWW Document]. Natl. Ocean. Atmospheric Adm. URL https://www.ncdc.noaa.gov/cdo-web/ (accessed 11.16.20).
National Interagency Fire Center, n.d. Total Wildland Fires and Acres (1926-2019) [WWW Document]. URL https://www.nifc.gov/fireInfo/fireInfo_stats_totalFires.html (accessed 2.5.21).
Natural Resources Conservation Service Oregon, n.d. Oregon SNOTEL Site Information [WWW Document]. US Dep. Agric. URL https://www.nrcs.usda.gov/wps/portal/nrcs/detail/or/snow/products/?cid=nrcs142p2_046159 (accessed 11.16.20).
Neary, D., Gottfried, G., Ffolliott, P., 2003. Post-wildfire watershed flood responses, in: Proceedings of the 2nd International Fire Ecology Conference. Orlando, Florida, pp. 16–20.
Neitsch, S.L., Arnold, J.G., Kiniry, J.R., Williams, J.R. 2011. Soil and water assessment tool theoretical documentation version 2009. Texas Water Resources Institute Technical Report No. 406 (p. 618). College Station, TX: Texas A&M University System.
Niemeyer, R.J., Bladon, K.D., Woodsmith, R.D., 2020. Long-term hydrologic recovery after wildfire and post-fire forest management in the interior Pacific Northwest. Hydrol. Process. 34, 1182–1197. https://doi.org/10.1002/hyp.13665.
Noske, P.J., Nyman, P., Lane, P.N.J., Sheridan, G.J., 2016. Effects of aridity in controlling the magnitude of runoff and erosion after wildfire. Water Resour. Res. 52, 4338–4357. https://doi.org/10.1002/2015WR017611.
Nyman, P., Sheridan, G., Lane, P.N.J., 2010. Synergistic effects of water repellency and macropore flow on the hydraulic conductivity of a burned forest soil, south-east Australia. Hydrol. Process. 24, 2871–2887. https://doi.org/10.1002/hyp.7701.
Onda, Y., Dietrich, W.E., Booker, F., 2008. Evolution of overland flow after a severe forest fire, Point Reyes, California. CATENA 72, 13–20. https://doi.org/10.1016/j.catena.2007.02.003.
Owens, P.N., Giles, T.R., Petticrew, E.L., Leggat, M.S., Moore, R.D., Eaton, B.C., 2013. Muted responses of streamflow and suspended sediment flux in a wildfire-affected watershed. Geomorphology, Process geomorphology and ecosystems: Disturbance regimes and interactions 202, 128–139. https://doi.org/10.1016/j.geomorph.2013.01.001.
Parson, A., Robichaud, P.R., Lewis, S.A., Napper, C., Clark, J.T., 2010. Field guide for mapping post-fire soil burn severity (No. RMRS-GTR-243). U.S. Department of Agriculture, Forest Service, Rocky Mountain Research Station, Ft. Collins, CO. doi: 10.2737/RMRS-GTR-243.
Paul, M.J., Meyer, J.L., 2001. Streams in the Urban Landscape. Annu. Rev. Ecol. Syst. 32, 333–365. https://doi.org/10.1146/annurev.ecolsys.32.081501.114040.
Pinheiro, J., Bates, D., DebRoy, S., Sarkar, D., R Core Team, 2020. nlme: Linear and Nonlinear Mixed Effects Models.
Poon, P.K., Kinoshita, A.M., 2018. Spatial and temporal evapotranspiration trends after wildfire in semi-arid landscapes. J. Hydrol. 559, 71–83. https://doi.org/10.1016/j.jhydrol.2018.02.023.
PRISM Climate Group, 2012. 30-Year Normals.
R Core Team, 2020. R: A language and environment for statistical computing.
Reilly, M.J., Dunn, C.J., Meigs, G.W., Spies, T.A., Kennedy, R.E., Bailey, J.D., Briggs, K., 2017. Contemporary patterns of fire extent and severity in forests of the Pacific Northwest, USA (1985–2010). Ecosphere 8, e01695.
Rengers, F.K., McGuire, L.A., Kean, J.W., Staley, D.M., Hobley, D.E.J., 2016. Model simulations of flood and debris flow timing in steep catchments after wildfire. Water Resour. Res. 52 (8), 6041–6061. https://doi.org/10.1002/2015wr018176.

Rhoades, C.C., Entwistle, D., Butler, D., 2011. The influence of wildfire extent and severity on streamwater chemistry, sediment and temperature following the Hayman Fire, Colorado. Int. J. Wildfire Sci. 20, 430–442.
Rhoades, C.C., Chow, A.T., Covino, T.P., Fegel, T.S., Pierson, D.N., Rhea, A.E., 2019. The legacy of a severe wildfire on stream nitrogen and carbon in headwater catchments. Ecosystems 22, 643–657. https://doi.org/10.1007/s10021-018-0293-6.
Robichaud, P.R., 2000. Fire effects on infiltration rates after prescribed fire in Northern Rocky Mountain forests, USA. J. Hydrol. 231–232, 220–229. https://doi.org/10.1016/S0022-1694(00)00196-7.
Robinne, F.-N., Hallema, D.W., Bladon, K.D., Flannigan, M.D., Boisramé, G., Bréthaut, C. M., Doerr, S.H., Baldassarre, G.D., Gallagher, L., Hohner, A.K., Khan, S.J., Kinoshita, A.M., Martin, D., Mordecai, R., Nunes, J.P., Nyman, P., Santín, C., Sheridan, G., Stoof, C.R., Thompson, M.P., Waddington, J.M., Wei, Y., 2021. Scientists' warning on extreme wildfire risks to water supply. Hydrol. Process. 35 https://doi.org/10.1002/hyp.14086.
Roche, J.W., Goulden, M.L., Bales, R.C., 2018. Estimating evapotranspiration change due to forest treatment and fire at the basin scale in the Sierra Nevada, California. Ecohydrology 11, e1978–e. https://doi.org/10.1002/eco.1978.
Rodrigues, E.L., Jacobi, C.M., Figueira, J.E.C., 2019. Wildfires and their impact on the water supply of a large neotropical metropolis: a simulation approach. Sci. Total Environ. 651, 1261–1271. https://doi.org/10.1016/j.scitotenv.2018.09.289.
Rust, A.J., Saxe, S., McCray, J., Rhoades, C.C., Hogue, T.S., 2019. Evaluating the factors responsible for post-fire water quality response in forests of the western USA. Int. J. Wildland Fire 28, 769–784. https://doi.org/10.1071/WF18191.
Ryberg, K.R., Vecchia, A.V., 2017. waterData: Retrieval, Analysis, and Anomaly Calculation of Daily Hydrologic Time Series Data.
Sahin, V., Hall, M.J., 1996. The effects of afforestation and deforestation on water yields. J. Hydrol. 178, 293–309. https://doi.org/10.1016/0022-1694(95)02825-0.
San-Miguel-Ayanz, J., Durrant, T., Boca, R., Mainanti, P., Libertá, G., Artés Vivancos, T., Oom, D., Branco, A., de Rigo, D., Ferrari, D., Pfeiffer, H., Grecchi, R., Nuijten, D., Leray, T., 2020. Forest Fires in Europe, Middle East and North Africa 2019 (Text No. EUR 30402 EN). Publications Office of the European Union.
Saxe, S., Hogue, T.S., Hay, L., 2018. Characterization and evaluation of controls on post-fire streamflow response across western US watersheds. Hydrol. Earth Syst. Sci. 22, 1221–1237. https://doi.org/10.5194/hess-22-1221-2018.
Scott, D.F., 1997. The contrasting effects of wildfire and clearfelling on the hydrology of a small catchment. Hydrol. Process. 11, 543–555. https://doi.org/10.1002/(SICI)1099-1085(199705)11:6<543::AID-HYP474>3.0.CO;2-J.
Seibert, J., McDonnell, J.J., Woodsmith, R.D., 2010. Effects of wildfire on catchment runoff response: a modelling approach to detect changes in snow-dominated forested catchments. Hydrol. Res. 41, 378–390. https://doi.org/10.2166/nh.2010.036.
Shakesby, R.A., 2011. Post-wildfire soil erosion in the Mediterranean: Review and future research directions. Earth-Sci. Rev. 105, 71–100. https://doi.org/10.1016/j.earscirev.2011.01.001.
Sheridan, G.J., Nyman, P., Langhans, C., Cawson, J., Noske, P.J., Oono, A., der Sant, R.V., Lane, P.N.J., Sheridan, G.J., Nyman, P., Langhans, C., Cawson, J., Noske, P.J., Oono, A., der Sant, R.V., Lane, P.N.J., 2015. Is aridity a high-order control on the hydro–geomorphic response of burned landscapes? Int. J. Wildland Fire 25, 262–267. https://doi.org/10.1071/WF14079.
Sidman, G., Guertin, D.P., Goodrich, D.C., Thoma, D., Falk, D., Burns, I.S., Sidman, G., Guertin, D.P., Goodrich, D.C., Thoma, D., Falk, D., Burns, I.S., 2015. A coupled modelling approach to assess the effect of fuel treatments on post-wildfire runoff and erosion. Int. J. Wildland Fire 25, 351–362. https://doi.org/10.1071/WF14058.
Smith, H.G., Sheridan, G.J., Lane, P.N.J., Nyman, P., Haydon, S., 2011. Wildfire effects on water quality in forest catchments: A review with implications for water supply. J. Hydrol. 396, 170–192. https://doi.org/10.1016/j.jhydrol.2010.10.043.
Snyder, K., Sullivan, T., Raymond, R., Moore, D., Gilbert, E., 2002. North Santiam River Watershed Assessment.
Soulis, K., Dercas, N., Valiantzas, J., 2012. Wildfires impact on hydrological response – the case of Lykorrema experimental watershed. Glob. Nest J. 14, 303–310.
Stoof, C.R., Wesseling, J.G., Ritsema, C.J., 2010. Effects of fire and ash on soil water retention. Geoderma 159, 276–285. https://doi.org/10.1016/j.geoderma.2010.08.002.
Stoof, C.R., Vervoort, R.W., Iwema, J., van den Elsen, E., Ferreira, A.J.D., Ritsema, C.J., 2012. Hydrological response of a small catchment burned by experimental fire. Hydrol. Earth Syst. Sci. 16, 267–285. https://doi.org/10.5194/hess-16-267-2012.
Strobl, C., Boulesteix, A.-L., Zeileis, A., Hothorn, T., 2007. Bias in random forest variable importance measures: Illustrations, sources and a solution. BMC Bioinformatics 8, 25. https://doi.org/10.1186/1471-2105-8-25.
Thomas, M.A., Rengers, F.K., Kean, J.W., McGuire, L.A., Staley, D.M., Barnhart, K.R., Ebel, B.A., 2021. Postwildfire soil-hydraulic recovery and the persistence of debris flow hazards. J. Geophys. Res. Earth Surf. 126 (6), e2021JF006091. doi: 10.1029/2021JF006091.
U.S. Army Corps of Engineers, n.d. Dataquery 2.0: Query Timeseries from USACE Northwestern Division [WWW Document]. URL https://www.nwd-wc.usace.army.mil/dd/common/dataquery/www/ (accessed 11.16.20).
Ulery, A.L., Graham, R.C., 1993. Forest fire effects on soil color and texture. Soil Sci. Soc. Am. J. 57, 135–140. https://doi.org/10.2136/sssaj1993.03615995005700010026x.
USDA Forest Service, n.d. BAER Road Treatment Tools – Curve Number Methods Supplement.
USDA Soil Conservation Service, 1986. Time of Concentration and Travel Time, in: Urban Hydrology for Small Watersheds, Technical Release.
USDA, 2013. Hydrologic Analyses of Post-Wildfire Conditions. Washington, DC.
Van der Sant, R.E., Nyman, P., Noske, P.J., Langhans, C., Lane, P.N.J., Sheridan, G.J., 2018. Quantifying relations between surface runoff and aridity after wildfire. Earth Surf. Process. Landf. 43, 2033–2044. https://doi.org/10.1002/esp.4370.
Wagenbrenner, J.W., Ebel, B.A., Bladon, K.D., Kinoshita, A.M., 2021. Post-wildfire hydrologic recovery in Mediterranean climates: a systematic review and case study to identify current knowledge and opportunities. J. Hydrol. https://doi.org/10.1016/j.jhydrol.2021.126772.
Wall, S.A., Roering, J.J., Rengers, F.K., 2020. Runoff-initiated post-fire debris flow Western Cascades, Oregon. Landslides 17, 1649–1661. https://doi.org/10.1007/s10346-020-01376-9.
Walsh, C.J., Roy, A.H., Feminella, J.W., Cottingham, P.D., Groffman, P.M., Morgan, R.P., 2005. The urban stream syndrome: current knowledge and the search for a cure. J. North Am. Benthol. Soc. 24, 706–723. https://doi.org/10.1899/04-028.1.
Warziniack, T., Sham, C.H., Morgan, R., Feferholtz, Y., 2017. Effect of forest cover on water treatment costs. Water Econ. Policy 03, 1750006. https://doi.org/10.1142/S2382624X17500060.
Westerling, A.L., 2016. Increasing western US forest wildfire activity: sensitivity to changes in the timing of spring. Philos. Trans. R. Soc. B Biol. Sci. 371, 20150178. https://doi.org/10.1098/rstb.2015.0178.
Williams, C.H.S., Silins, U., Spencer, S.A., Wagner, M.J., Stone, M., Emelko, M.B., 2019. Net precipitation in burned and unburned subalpine forest stands after wildfire in the northern Rocky Mountains. Int. J. Wildland Fire 28, 750–760. https://doi.org/10.1071/WF18181.
Wine, M.L., Cadol, D., 2016. Hydrologic effects of large southwestern USA wildfires significantly increase regional water supply: fact or fiction? Environ. Res. Lett. 11, 085006 https://doi.org/10.1088/1748-9326/11/8/085006.
World Economic Forum, 2015. Global Risks 2015, 10th ed. World Economic Forum, Geneva, Switzerland.
Wu, J., Baartman, J.E.M., Nunes, J.P., 2021. Comparing the impacts of wildfire and meteorological variability on hydrological and erosion responses in a Mediterranean catchment. Land Degrad. Dev. 32, 640–653. https://doi.org/10.1002/ldr.3732.
Xu, Y., 2020. hyfo: Hydrology and Climate Forecasting.
Xue, L., Li, Q., Chen, H., 2014. Effects of a wildfire on selected physical, chemical and biochemical soil properties in a Pinus massoniana forest in South China. Forests 5, 2947–2966. https://doi.org/10.3390/f5122947.
Zaremehrjardy, M., Razavi, S., Faramarzi, M., 2021. Assessment of the cascade of uncertainty in future snow depth projections across watersheds of mountainous, foothill, and plain areas in northern latitudes. J. Hydrol. 598, 125735 https://doi.org/10.1016/j.jhydrol.2020.125735.
Johnson, S., Wondzell, S., Rothacher, J., 2020. Stream discharge in gaged watersheds at the HJ Andrews Experimental Forest, 1949 to present. Long-Term Ecological Research. Forest Science Data Bank, Corvallis, OR. [Database]. Available: http://andlter.forestry.oregonstate.edu/data/abstract.aspx?dbcode=HF004. https://doi.org/10.6073/pasta/0066d6b04e736af5f234d95d97ee84f3.